AFRL-RH-WP-TR-2010-0143

METABONOMICS APPROACH TO BIOMARKER DISCOVERY

Volume VI: Dose and Time Response of Liver Toxicant

Nicholas DelRaso
Deirdre Mahle
Randall Rietcheck
Jessica Young
Biosciences and Protection Division
Applied Biotechnology Branch

Nicholas Reo
Michael Raymer
Andrew Neuforth
Wright State University, Dayton OH

Harry Luithardt
Solutions Labs Inc., Cambridge MA

Nestor Tarragona
Tufts Medical School, Boston MA

Mark Westrick
Dept of Chemistry, US Air Force Academy CO

May 2009

Final Report for October 2005 to April 2009

Air Force Research Laboratory
711th Human Performance Wing
Human Effectiveness Directorate
Biosciences and Performance Division
Applied Biotechnology Branch
Wright-Patterson AFB, OH 45433

NOTICE

Using Government drawings, specifications, or other data included in this document for any purpose other than Government procurement does not in any way obligate the U.S. Government. The fact that the Government formulated or supplied the drawings, specifications, or other data does not license the holder or any other person or corporation; or convey any rights or permission to manufacture, use, or sell any patented invention that may relate to them.

This report was cleared for public release by the 88th Air Base Wing Public Affairs Office and is available to the general public, including foreign nationals. Copies may be obtained from the Defense Technical Information Center (DTIC) (http://www.dtic.mil).

AFRL-RH-WP-TR-2010-0143

THIS REPORT HAS BEEN REVIEWED AND IS APPROVED FOR PUBLICATION IN ACCORDANCE WITH ASSIGNED DISTRIBUTION STATEMENT.

//SIGNED//
REBECCA GULLEDGE, Work Unit Manager
Applied Biotechnology Branch

//SIGNED//
MARK M. HOFFMAN, Deputy Chief
Biosciences and Performance Division
Human Effectiveness Directorate
711th Human Performance Wing
Air Force Research Laboratory

This report is published in the interest of scientific and technical information exchange, and its publication does not constitute the Government's approval or disapproval of its ideas or findings.

REPORT DOCUMENTATION PAGE

Form Approved
OMB No. 0704-0188

1. REPORT DATE *(DD-MM-YYYY)*	2. REPORT TYPE	3. DATES COVERED *(From - To)*
30-05-2009	Final	1Oct 2005 – 30 Apr 2009

4. TITLE AND SUBTITLE

Metabonomics Approach to Biomarker Discovery: Dose and Time Response of Liver Toxicant

5a. CONTRACT NUMBER

5b. GRANT NUMBER

5c. PROGRAM ELEMENT NUMBER
62202F

6. AUTHOR(S)

DelRaso, Nicholas[1]; Mahle, Deirdre[1]; Rietcheck, Randall[1]; Young, Jessica[1]; Reo, Nicholas[2], Raymer, Michael[2]; Neuforth, Andrew[2]; Luithardt, Harry[3]; Tarragona, Nestor[4]; Westrick, Mark[5]

5d. PROJECT NUMBER
7184

5e. TASK NUMBER
D4

5f. WORK UNIT NUMBER
7184D405

7. PERFORMING ORGANIZATION NAME(S) AND ADDRESS(ES)
[2]Wright State University, Dayton OH 45429
[3]Solutions Labs, 400 Technology Square, Cambridge MA 02139-3583
[4]School of Medicine, Tufts Medical Center, 136 Harrison Ave, Boston MA 02110
[5]Dept of Chemistry, 2354 Faculty Dr, US Air Force Academy CO 80840

8. PERFORMING ORGANIZATION REPORT NUMBER

9. SPONSORING / MONITORING AGENCY NAME(S) AND ADDRESS(ES)
[1]Air Force Materiel Command
Air Force Research Laboratory
711th Human Performance Wing
Human Effectiveness Directorate
Biosciences and Performance Division
Applied Biotechnology Branch
Wright-Patterson AFB OH 45433-5707

10. SPONSOR/MONITOR'S ACRONYM(S)
711 HPW/RHPB

11. SPONSOR/MONITOR'S REPORT NUMBER(S)
AFRL-RH-WP-TR-2010-0143

12. DISTRIBUTION / AVAILABILITY STATEMENT
Distribution A: Approved for public release; distribution unlimited.

13. SUPPLEMENTARY NOTES

14. ABSTRACT
The work described in the following report was initiated to investigate the possibility of using novel biotechnologies for the discovery, down-selection, and pre-validation of biomarkers of toxic substance effects within the warfighter prior to health and operational performance decrement. Using the biotechnology of metabonomics, this effort focused on using nuclear magnetic resonance (NMR) spectroscopy and ultra pressure liquid chromatography mass spectrometry (UPLC/MS) for identification of liver-selective toxic effects following exposure to a known hepatotoxicant (alpha-naphthylisothiocyanate; ANIT) that induces cholestasis. Urine samples were analyzed by NMR spectroscopy and UPLC/MS and the data processed and analyzed by principal component analysis, linear discriminant analysis, and hierarchical clustering analysis. NMR- and UPLC/MS-based urinary metabonomics were sensitive enough to detect ANIT-induced toxic effects with respect to both dose and time. Understanding the cellular response to chemical exposure at the molecular level will not only facilitate the elucidation of the mechanism of chemical toxicity, but also allow accurate prediction of chemical toxicity and phenotypic outcome. Ultimately, this will lead to the identification of novel biomarkers for rapid monitoring and prediction of health hazards to the warfighter associated with chemical exposure.

15. SUBJECT TERMS
metabonomics, biomarker, exposure, liver, alpha-naphthylisothiocyanate, toxicity, NMR, UPLC/MS, cholestasis, principal components, linear discriminant, hierarchical clustering

16. SECURITY CLASSIFICATION OF:			17. LIMITATION OF ABSTRACT	18. NUMBER OF PAGES	19a. NAME OF RESPONSIBLE PERSON
a. REPORT	b. ABSTRACT	c. THIS PAGE			Rebecca Gulledge
U	U	U	SAR	71	19b. TELEPHONE NUMBER *(include area code)* NA

Standard Form 298 (Rev. 8-98)
Prescribed by ANSI Std. 239.18

THIS PAGE INTENTIONALLY LEFT BLANK.

TABLE OF CONTENTS

Section **Page**

LIST OF FIGURES

Figure **Page**

LIST OF TABLES

Table **Page**

PREFACE

This research was accomplished at the Applied Biotechnology Branch, Human Effectiveness Directorate of the 711th Human Performance Wing (711 HPW/RHPB) of the Air Force Research Laboratory, Wright-Patterson AFB, OH, under Dr. John J. Schlager, Branch Chief. This work unit report was written for AFRL Work Unit 7184D405.

All studies involving animals were approved by the Wright-Patterson Institutional Animal Care and Use Committee, and were conducted in a facility accredited by the Association for the Assessment and Accreditation of Laboratory Animal Care, International, in accordance with the *Guide for the Care and Use of Laboratory Animals* (1996).

ACKNOWLEDGEMENTS

This work was supported by grants to Wright State University from the Air Force Research Laboratory, Human Effectiveness Directorate, Biotechnology Branch (AFRL/RHPB), Man-tech Environmental Technology, Inc. (Contract No. ManTech/WBI-002), Alion Science and Technology (Contract No. SUB1174146RB), and The Henry M Jackson Foundation for Advancement of Military Medicine, Inc. (Contract No.132633). Work was also supported by Air Force SBIR funding to Solutions Labs, Cambridge, MA (Contract No. FA-8650-06-C-6754).

SUMMARY

The work described in this report was initiated to identify, down-select, and pre-validate biomarkers of toxic substance effects on a selected target-organ in a rat animal model that may occur within the warfighter prior to inducing a reduction in health or operational performance. Using the biotechnology of metabonomics (NMR-based and UPLC/MS-based), this research effort focused on identification of potential liver-selective markers of toxic effects induced by the cholestatic agent alpha-naphthylisothiocyanate (ANIT) in rats that may be extrapolated to identifying warfighter organ-specific chemical exposure effects before significant decrement to mission performance or latent induction of an organ-targeted disease process is observed. Results of the present study indicated that NMR and UPLC/MS analysis of rodent urine samples could detect changes in metabolite profiles, using either simple statistics ($p<0.05$) or computer-based multi-dimensional statistical analysis, following exposure to ANIT at levels below that indicative of toxicity by traditional clinical and histopathological methods.

THIS PAGE INTENTIONALLY LEFT BLANK

1.0 INTRODUCTION

Metabonomics can be viewed as a systems biology approach that integrates divergent effects that occur over both time and space (Fernie et al., 2004; Lindon[1] et al., 2004). Metabonomics is defined as "the quantitative measurement of the time-related multiparametric metabolic response of living organisms to pathophysiological stimuli or genetic modification" (Nicholson et al., 1999). This term is derived from the Greek roots "meta" (change) and "nomos" (regularity and order); referring to the ability of chemometric models to classify changes in metabolism (Lindon[1] et al., 2004). This biotechnology was pioneered by Jeremy Nicholson, Elaine Holmes and John Lindon in the late 1990s at the Imperial College in London (Nicholson et al., 1999). The field of metabonomics is concerned with the study of fixed cellular and biofluid concentrations of endogenous metabolites, as well as dynamic metabolite fluctuations, exogenous species, and molecules that arise from chemical rather than enzymatic processing (Lindon et al., 2003). Use of metabonomics has increased the ability to identify and characterize the site and extent of cellular injury earlier and more accurately than traditional clinical chemistry or histopathology. This technique can identify metabolic markers of toxicity, progression of injury, response to treatment and recovery from insult in easily collected biofluids such as blood and urine (Lenz et al., 2003; Holmes et al., 2000; Lindon et al., 1999; Anthony[1] et al., 1994; Holmes[1] et al., 1992; Holmes[2] et al., 1992). Furthermore, extensive literature exists on the use of metabonomics procedures to evaluate chemical/drug induced target-organ toxicity (Nicholson et al., 2002; Robertson et al., 2000; Holmes and Shockcor, 2000; Beckwith-Hall et al., 1998; Holmes et al., 1998a; Holmes[1] et al., 1998; Anthony[2] et al., 1994).

A frequent misconception is that metabonomics is based primarily on nuclear magnetic resonance spectroscopy (NMR)-derived data. In theory, any technology that has the capacity to generate comprehensive metabolite measurements can be used for metabonomics. The most common analytical platforms used today in metabonomics are proton NMR and mass spectroscopy coupled to ultra pressure liquid chromatography (UPLC/MS) or gas chromatography. The advantages of NMR-based metabonomics include nondestructive analysis, applicable to intact biomaterial, and information-rich with respect to determinations of molecular

structure, especially in complex mixtures. The non-selectivity, lack of sample bias and reproducibility of NMR is of critical importance when considering toxicological screening applications (Keun et al. 2002). Changes in NMR-derived urinary metabolite levels have proven to be a sensitive indicator of chemical-induced toxicity (Waters et al., 2002; Nicholson, et al., 2002; Reo, 2002; Robertson et al., 2000; Holmes and Shockcor, 2000; Anthony[2] et al., 1994).

Mass spectroscopy offers the ability to detect chemical classes not detected by NMR (i.e. sulfates), and the capability to detect lower abundance metabolites with little sample processing (Dunn and Ellis, 2005). This is of critical importance if one is searching for novel biomarkers of toxicity or disease. Urinary metabolite analysis using UPLC/MS has also been used to profile chemical-induced toxicity (La et al., 2005). It is clear to see that UPLC/MS is complimentary to NMR data and facilitates metabolite identification.

α-Naphthylisothiocyanate (ANIT) is a cholestatic hepatotoxin that has been used as a model compound for developing metabonomic techniques. ANIT is known to induce hepatocellular and biliary epithelial cell necrosis, bile duct obstruction and biliary cell hyperplasia in rats (Plaa, and Priestly, 1976; Goldfarb et al., 1962). In addition, ANIT has been thoroughly characterized biochemically with respect to dose and time (Uchida et al., 2002; Chisholm and Dolphin, 1996). Much is known about the systemic response to ANIT exposure, such as the increase in plasma levels of bile acid, cholesterol and phospholipids in male rats after a single 100 mg/kg ANIT oral exposure (Chisholm and Dolphin, 1996). Therefore, ANIT is an ideal compound to evaluate the sensitivity of NMR-based metabonomics and to assess the time- and dose-response relationships of chemically induced toxicity.

The extent of toxicity is dependent on both dose and time (Rozman and Doull, 1998). Therefore, the use of a metabonomics approach for toxicological assessment must go beyond simply looking for differences between experimental control and exposed animals at toxic doses. A number of reviews on the role of metabonomics in toxicology have been published (Robertson, 2005; Lindon[1] et al., 2004; Lindon[2] et al., 2004; Lindon et al., 2003; Shockcor and Holmes, 2002; Reo, 2002). For a description of the severity of biological effects and a valid

identification of true biomarkers of toxicity it is critical to consider both time and dose as factors of toxicity. The objective of this study was to investigate the dose and time dependent responses of the urinary metabolic profile following an acute exposure to the hepatotoxicant ANIT in F344 rats over four days. The present study included six doses of ANIT ranging from 0.1 to 100 mg/kg. This range represents dosages that are non-toxic to overtly toxic, as determined by clinical chemistry and histopathology. The results of the present study show that proton NMR and UPLC/MS analysis of rat urine were sensitive enough to reveal the relationship between dose and time, even at non-toxic dose levels, a key step toward biomarker discovery.

2.0 METHODS

2.1 Animals

All protocols for handling laboratory animals were approved by the Wright-Patterson Institutional Animal Care and Use Committee (IACUC) and meet appropriate Federal guidelines. Male Fischer 344 rats (CDFR(F344)/CrlBR; 200-250 g) were used for all experiments. Animals were obtained from Charles Rivers Laboratory (Raleigh, NC) with surgically implanted jugular vein catheters. Animals were transferred into metabolism cages (Lab Products, Inc, Seaford, DE) five days prior to the start of the study to allow acclimation to the new environment. All animals were housed individually in metabolism cages for the duration of the experiment, and were given *ad libitum* access to food (Purina Certified Rat Chow # 5002) and fresh conditioned reverse osmosis water. The housing environment was maintained on a 12 hour light-darkness cycle at 25 °C, and all animals were examined by Vivarium personnel twice daily. Animals were given a single administration, via oral gavage at 10 mL/kg, of ANIT in corn oil vehicle at one of the following doses: 0.1, 1, 10, 20, 50 or 100 mg/kg. Control animals received corn oil only at 10 mL/kg. Separate control groups were included for each ANIT dose study. The sample sizes (n-values) are given in the legend to Figures 2 and 3. Blood samples were collected 10 d pre-dose and 24 h post-dose from the jugular vein catheter, and at termination on day-4 via the inferior vena cava. Saline-heparin lock solution was removed from catheters prior to withdrawing 1.4 mL of blood for plasma collection. The first 100 μL of blood collected was discarded. Urine samples were collected daily into 50 mL collection tubes, containing 1 mL of 1% sodium azide and were chilled on dry ice. All urine samples were stored at -20 °C prior to analysis by NMR spectroscopy. Rats were sacrificed by carbon dioxide inhalation four days post-dose, and livers were removed and fixed for histopathology as described below.

2.2 Plasma Biochemistry

Rat blood was collected pre-dose, 24 h post-dose and at the time the animals were euthanized. Plasma was separated from the cellular components by centrifugation and frozen at -80 °C until analyzed. Animal plasma samples were analyzed for aspartate aminotransferase

(AST), alanine aminotransferase (ALT), alkaline phosphatase (ALKP), urea nitrogen (BUN), creatine (CREA) and total protein (TP) activities using a Vet Test (Westbrook, ME) clinical chemistry analyzer. All clinical chemistry assays were performed in accordance with manufacturer's protocols for this clinical chemistry analyzer.

2.3 Histopathology

Target tissues (i.e. liver and kidney) were collected at sacrifice, fixed in 10% formalin and processed in accordance with accepted pathological protocols. Briefly, tissues were embedded in paraffin, sliced and stained with hematoxylin and eosin. Sections were evaluated by a staff veterinarian pathologist by light microscopy for mononuclear cellular infiltration, biliary hyperplasia/hypertrophy, portal edema and portal inflammation. Severity was graded on a scale of one to five with one being minimal and five being severe.

2.4 NMR Metabonomics

2.4.1 Urine Sample Processing.

Urine samples for NMR analysis were prepared as described by Robertson et al. (2000) and modified as follows. Urine samples were thawed at 4 °C overnight, and then equilibrated to room temperature just prior to NMR sample preparation. A 600 µL aliquot of urine was transferred to a 1.5 mL Eppendorf tube, mixed with 300 µL of phosphate buffer (0.2 M monosodium phosphate and 0.2 M disodium phosphate, pH 7.4), and allowed to equilibrate for ten minutes. Samples were then centrifuged at 5000 rpm for ten minutes to remove any particulate matter, and 550 µL of supernanant was transferred to a 5 mm NMR tube. An internal standard consisting of 150 µL of trimethylsilylpropionic (2, 2, 3, 3 d_4) acid (TSP) dissolved in deuterium oxide was added at a final concentration of 2 mM.

2.4.2 NMR Spectroscopy.

Proton NMR spectra were acquired on a Varian INOVA operating at 600 MHz and a probe temperature of 25 °C. Water suppression was achieved using the first increment of a NOESY pulse sequence, which incorporated saturating irradiation (on resonance for water) during the relaxation delay (2 s pre-saturation) and the mixing time. The urine sample acquisition parameters included a mixing time of 38 ms and a 4.0 s acquisition time. The data were signal averaged over 64 transients using an interpulse delay of 9.05 s.

2.4.3 Multivariate Statistical Analysis.

Proton NMR spectral data were processed using Varian software and employing exponential multiplication (0.3 Hz line-broadening), Fourier transformation, and baseline flattening (fifth-order polynomial and spline fitting routines). Spectra were subdivided into 280 regions (bins) of 0.04 ppm width for integration using Varian Binning software. The residual water signal (~4.8 ppm) and the urea signal in urine spectra (~5.8 ppm) were excluded from the analyses. Integrated bin areas were transferred to an Excel file and normalized to the TSP signal intensity. A second normalization was performed by summing 256 bins over the entire metabolite range, which excludes the region of TSP signal (0.53 to -0.28 ppm). These 256 'sum normalized' bins were used as input to principal component analysis (PCA) and linear discriminant analysis (LDA) performed using MatLab 7.0. Pattern recognition method (PCA scores plots) was used to enable data visualization and help to identify interesting samples and time-points such as: outliers; time of maximum biochemical impact; average time to recovery; rats showing different rates of recovery; etc. Orthogonal Partial Least Squares-Discriminant Analysis (OPLS-DA) was used to enable classification into specific groups. The OPLS correlation coefficients were then used to weight and rank the salient spectral peaks (metabolites signals). Various quality metrics were used to validate and provide a level of statistical confidence to the results (i.e., Q2, R2, accuracy, leave-one-out cross validation, bin-by-bin t-tests, etc). Bin-by-bin t-test was used to identify significant spectral features that showed similar patterns of change across the study time-course. Statistical group comparisons and hierarchal cluster analysis were conducted to discern similar and dissimilar spectral features between exposed and control animals. Data from individual animals were analyzed as a function of time, as each animal served as its own control. The salient spectral resonances were assigned to metabolites using Chenomx 5.1 software, on-line NMR databases (i.e., mmcd.nmrfam.wisc.edu; U. Wisconsin, etc), and by "spiking" samples with known compounds, if necessary.

2.5 UPLC/MS Metabonomics

High-performance liquid chromatography based metabonomics analysis was performed using the Waters Acquity® ultra-performance liquid chromatography coupled to a Waters Q-ToF® hybrid tandem quadrupole/time of flight mass spectrometer (UPLC/MS) equipped with an electrospray source operating in either positive or negative ion mode, and an integrated Lockspray interface for exact mass measurements and with extended dynamic range. Prior to analysis by UPLC/MS, rat urine aliquots of 1 ml were centrifuged at 14000 x g for 10 minutes at 4 C to remove insoluble material, the supernatant was filtered using a 0.22μm PTFE filter, the supernatant was then diluted 1:3 in water and injected into an LC/ESI/Q-ToF/MS without further manipulation. Arrangements were made to use the UPLC-MS Waters metabolic profiling platform at the Laboratory for Translational Medicine at Harvard Medical School, Cambridge, MA, under the direction of Dr. Nestor Tarragona. This platform provides both extremely high chromatographic resolution and reproducibility in combination with high mass accuracy (<10 ppm) and an integrated software suite for the identification of potential metabolite biomarkers via the Waters Markerlynx package.

2.5.1 UPLC-MS Conditions:

1) Stationary phase: 2.1 x 100 mm 1.7 μm UPLC C 18
2) Mobile Phase was different in positive and negative mode.
   - For W positive: Solvent A: 0.1% Formic Acid in Water. Solvent B: 0.1% Formic Acid in Acetonitrile.
   - For W negative: Solvent A: 0.1% Ammonium Acetate in Water. Solvent B: 0.1% Ammonium Acetate in Acetonitrile.

3) Gradient

Time (min)	% Solvent A	% Solvent B
0	100	0
5	80	20
10	10	90

4) Flow rate: 0.4 ml/min
5) Injection volume: 10 µl

The mass spectrometer was equipped with an electrospray source, operating in either positive or negative ion mode (W mode), and an integrated Lockspray interface. The Internal lock masses were 50 fmol/µl Leucine Enkephalin and 500 fmol/µl of reserpine in Water-Methanol (1:1). Cone Voltage was set to 15 V, de-solvation and source temperature to 300 ˚C and 100 respectively. Mass acquisition Range was between 70-1000 m/z

2.6 Data Analysis and Metabolite Identification

UPLC/MS data was analyzed by Dr Harry Luithart of Solutions Labs, Cambridge, MA, using the Waters MarkerLynx Applications Manager (latest version). MarkerLynx software incorporates a peak de-convolution package that allowed detection and retention time alignment of the peaks eluting in each chromatogram. The data was combined into a single matrix by aligning peaks with the same mass/retention time pair together from each data file in the dataset, along with their associated intensities. Data was also de-isotoped prior to subsequent analysis. PCA of resulting data matrix shows outstanding clustering in a scores plot of the first two components.

2.6.1 Data Preprocessing for Pattern Recognition.

The data matrix generated by MarkerLynx is extremely sparse, and each zero intensity reported was actually a reading made below a lower bound threshold (i.e. they are unreliable values). Therefore, the original set of approximately 14,000 variables was subjected to a filtering procedure aimed at retaining only variables that have a high probability of appearing in a reproducible fashion in follow-up studies. Our filtering method is a modification of procedures recommended by Smilde et al. (2005). We imposed an "80% rule" in which an ionic species must have at least 80% non-zero readings in at least one of the five data groups (i.e. pre-dose, 0 mg/kg 24 and 48 hours, 50 mg/kg 24 and 48 hours). If this criterion is not met, then a variable is removed from the data matrix, and the final data matrix ends up containing approximately 4000 variables. This reduced data matrix is normalized using the sum of the individual sample intensities, and the variables are subsequently scaled using a unit variance transform. The effect of using a logarithmic transform prior to scaling was also considered.

2.6.2 UPLC/MS Chemometric Analysis.

Data for time 48 hours post-exposure was considered in a two group analysis using PLS-DA. After removing any outliers, over 99% variance was captured in the first component of the Y-block, and the first component of the X-block captured approximately 45% of its variation. Thus, first component loadings may be used to rank variables with respect to group separation. By studying the magnitude of loadings and trends plots of ion species across samples, it became apparent that up to 1000 variables might be important for separating the two groups.

3.0 RESULTS AND DISCUSSION

3.1 Clinical Chemistry and Histopathology

Clinical chemistry analyses indicated that rats exposed to 100 mg/kg ANIT showed significant ($p \leq 0.05$) elevation of liver transaminases (AST and ALT) and ALKP throughout the four-day study period when compared to control (Table 1). Blood clinical chemistry data for the two-day study involving 50 mg/kg ANIT and vehicle controls are shown in Table 2.

Table 1: Plasma enzyme activity assays for alkaline phosphatase (ALKP), alanine aminotransferase (ALT), and aspartate aminotransferase (ASP) in rats treated with a single dose of ANIT or corn oil (vehicle control) at day-zero.

Values are Mean ± SD (n=5).

ANIT Dose (mg/kg)	ALKP (U/L)		ALT (U/L)		AST (U/L)	
	Day-1	Day-4	Day-1	Day-4	Day-1	Day-4
Control (corn oil)	280 ± 54	327 ± 42	38 ± 8	40 ± 11	82 ± 18	88 ± 18
100	370 ± 22*	609 ± 155*	152 ± 60*	125 ± 37*	278 ± 142*	229 ± 101*
50	380 ± 115	397 ± 50	232 ± 154*	56 ± 16	552 ± 98*	73 ±13
20	254 ± 56	224 ± 46	25 ± 7	51 ± 9	61 ± 14	74 ± 10
10	291 ± 20	332 ± 127	38 ± 6	36 ± 9	79 ± 10	88 ± 16
1	315 ± 22	293 ± 16	41 ± 11	39 ± 6	88 ± 23	68 ± 3
0.1	227 ± 16	188 ± 22	29 ± 6	39 ± 1	70 ± 13	67 ± 6

($p \leq 0.05$).

Table 2: Measures of plasma enzymes in rats treated with a single dose of 50 mg/kg ANIT or corn oil (vehicle control) at day-zero.

Values are Mean ± SD (n = 5 – 8). The asterisk denotes a significant difference from control at the corresponding time (p≤0.05). Abbreviations are given in Table 1.

Group	ALKP (U/L)		ALT (U/L)		AST (U/L)	
	Day-1	Day-2	Day-1	Day-2	Day-1	Day-2
Control (Corn Oil)	241 ± 28	281 ± 103	24 ± 2	37 ± 21	53 ± 3	80 ± 14
ANIT (50 mg/kg)	248 ± 27	525 ± 118*	183 ± 80*	546 ± 88*	333 ± 144*	628 ± 116*

Rats exposed to 50 mg/kg ANIT showed a significant elevation in liver transaminases at days one and two post-exposure, but recovered to normal levels by day-4 (Tables 1 and 2). ALKP in this group was significantly elevated at day-two, but not days one or four. Rats exposed to ANIT concentrations less than 50 mg/kg did not demonstrate any significant change in liver enzymes throughout the study. The highest ANIT dose tested that did not induce any significant clinical effects on the liver was 20 mg/kg. Histopathological examination of the liver indicated that no significant changes occurred in any of the animals exposed to ANIT at ≤20 mg/kg. However, significant histopathological changes were observed in rats exposed to ANIT at 50 mg/kg or higher at four days post-dose (Table 3). For the 50 mg/kg ANIT study terminated at two days post-exposure, histopathology of livers yielded similar severity scores as the four-day study for this dose group (minimal to mild effects with severity scores of 1-2; data not shown).

Table 3: Liver histopathology scores in rats at four days post-dose with either corn oil (control) or ANIT at doses indicated.

Severity scores for individual rats are: 0 = no lesion, 1 = minimal, 2 = mild, 3 = moderate, 4 = marked and 5 = severe. The gray shading indicates data are significantly different from control (2-tailed Wilcoxon Rank Sum test, p ≤ 0.05).

Liver Index	Control	ANIT Dose (mg/kg)					
	Corn Oil	0.1	1	10	20	50	100
Mononuclear Cell Infiltrates, Random	0,0,0,0,0,0,0,1,1,1	0,0,1	0,0,0	0,0,1	0,0,0,0	0,0,0,0	0,0,0,0,0,0,0,0,0,0
Biliary Hyperplasia/ Hypertrophy	0,0,0,0,0,0,0,0,0,0	0,0,1	0,0,0	0,0,0	0,0,1,2	0,1,1,2	1,1,2,2,2,2,2,2,2,2
Portal Edema	0,0,0,0,0,0,0,0,0,1	0,0,1	0,1,1	0,0,1	0,0,1,2	1,1,1,2	0,0,0,0,0,0,1,1,1,1
Portal Inflammation	0,0,0,0,0,0,0,0,1,2	0,0,1	0,0,0	0,0,2	0,0,1,2	1,1,1,2	0,0,1,2,2,2,2,2,2,2

3.2 NMR Spectroscopy of Urine Samples

The NMR spectra shown in Figure 1 represent the changes in endogenous components of urinary metabolites observed over time in a rat given a single oral dose of 100 mg/kg ANIT. The pre-dose urine NMR spectrum is representative of naïve animals. Twenty-four hours following exposure to 100 mg/kg ANIT the intensities of resonances from α-ketoglutarate, citrate, and hippurate were clearly reduced. By day-two, these signals continued to decrease, along with an increase in creatine. NMR spectra for this ANIT dose group returned towards the pre-dose profile by day-four (as observed by PCA; spectra not shown). More details regarding the metabolic changes are presented in *LDA Results* below.

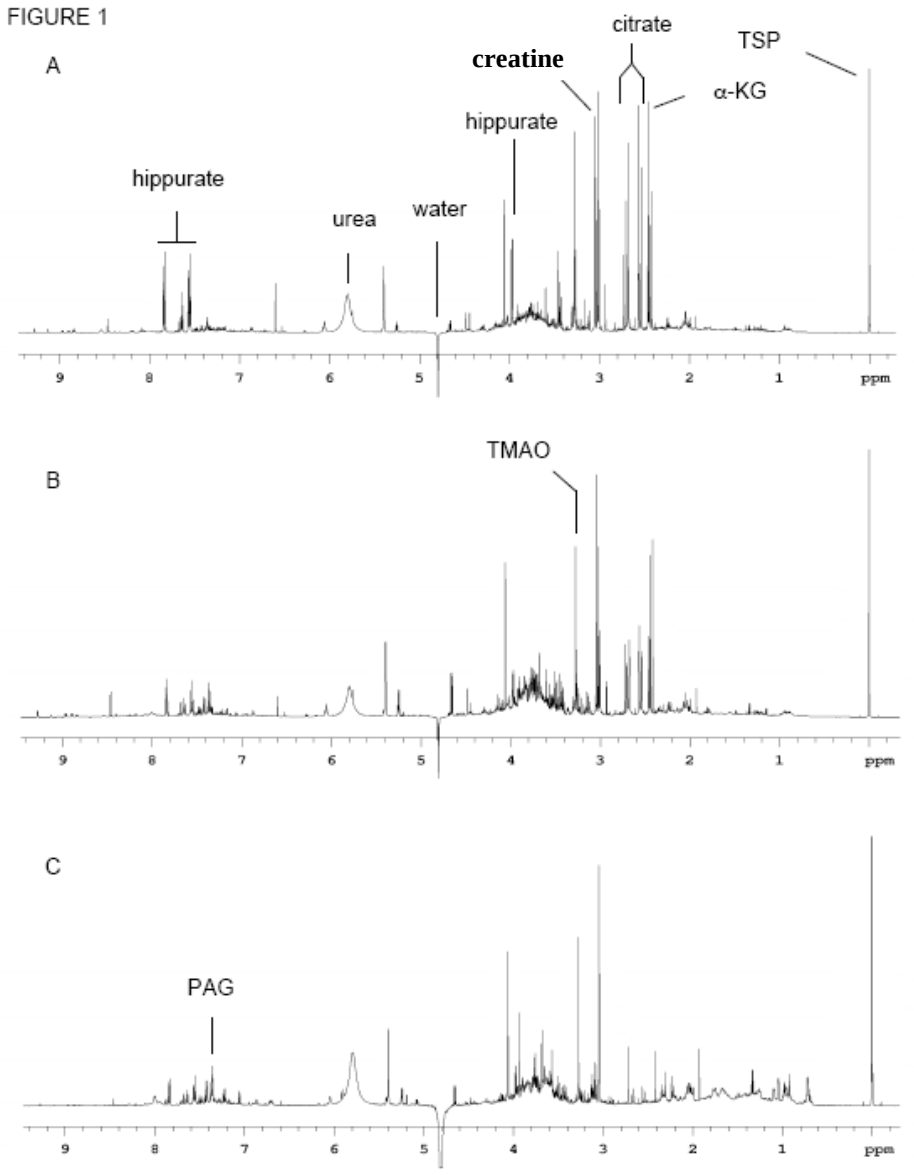

Figure 1. Representative 600 MHz 1H NMR urine spectra from a rat dosed with 100 mg/kg ANIT showing changes from (A) pre-dose to (B) day-one and (C) day-two post-dose. *Major analytes that were affected by ANIT treatment are labeled in the aliphatic region (2.0 to 4.0 ppm). TSP, water and urea are labeled for reference. See text for abbreviations.*

3.2.1 PCA Results.

The 256 bin intensities from each urine spectrum provided multivariate data input to PCA, which was conducted for each dose group in combination with the vehicle-treated control group. The results are presented graphically in Figures 2 - 4.

Figure 2 shows PCA scores plots (PC1 vs. PC2) for each dose group versus controls as a function of time from pre-dose (d0) to day-four post-dose (d4). The use of the first two principal components (PCs) was sufficient to demonstrate pattern separation between treatment groups. For all analyses, the first two PCs explained >50% of the variance in the data. Data points represent the mean values for the PCs at each time point, and the ellipse encircling each point depicts the ±standard error (SE) boundaries. We chose to plot only the mean values because graphing all sample points results in plots that are cluttered and difficult to interpret, especially for the lower dose groups, which show little separation. The spread in data points, however, is shown in Figure 3 for the 50 mg/kg ANIT dose group. The control group in these plots is composed of all vehicle control animals collectively from each dose study (n=22 at days 0, 1, 2; but n=14 at days three and four). The larger sample size for days zero-two results from the 8 additional animals included from the two-day ANIT study (see Experimental Procedures).

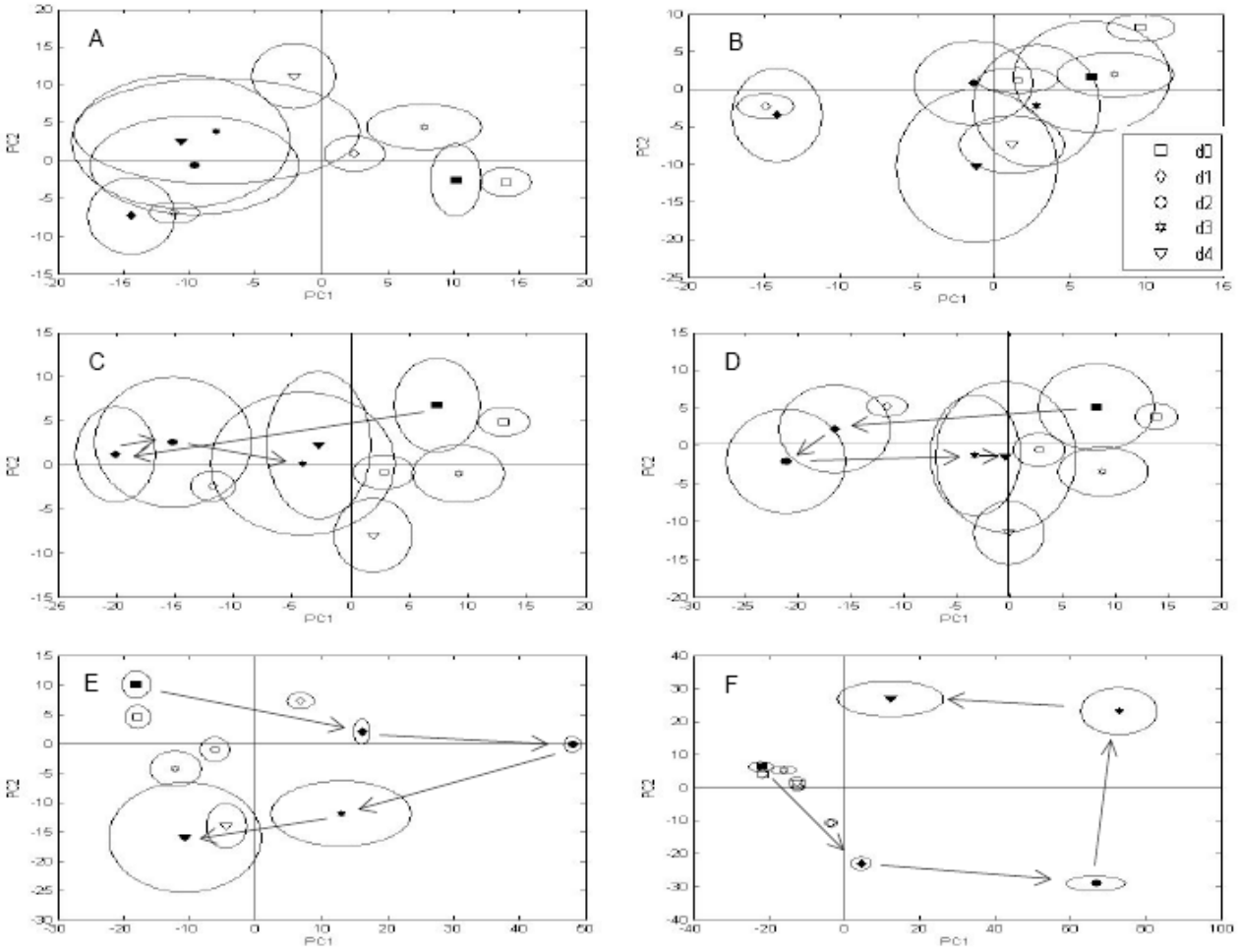

Figure 2. PCA of each ANIT dose as a function of time from day-zero (pre-dose) to day-four post-dose (see legend in panel B).

Treated (filled symbols) and vehicle-treated control (open symbols) data are plotted as the mean value for the first two principal components (PC1 vs. PC2) with an ellipse indicating the ±SE in both dimensions. Corresponding control animals were included with each ANIT dose experiment, but these PCA included all controls (n=14 or 22 depending upon the time point; see below) versus each individual ANIT dose group as follows: (A) 0.1 mg/kg (n=6); (B) 1 mg/kg (n=6); (C) 10 mg/kg (n=7); (D) 20 mg/kg (n=7); (E) 50 mg/kg (n=13 for d0, d1, and d2, but n=5 for d3 and d4); and (F) 100 mg/kg (n=9). The n-values for the control group (n=22 for d0, d1, and d2; n=14 for d3 and d4) and the 50 mg/kg group vary at different times since they included

an additional separate cohort of animals, which were sacrificed at 2-days post-dose. PCA vector trajectories (arrows in panels C-F) represent induction of ANIT-induced changes in mapping position with respect to time. Note the different scales between dose groups indicating the range in data values (i.e., ≤20 mg/kg versus 50 mg/kg versus 100 mg/kg).

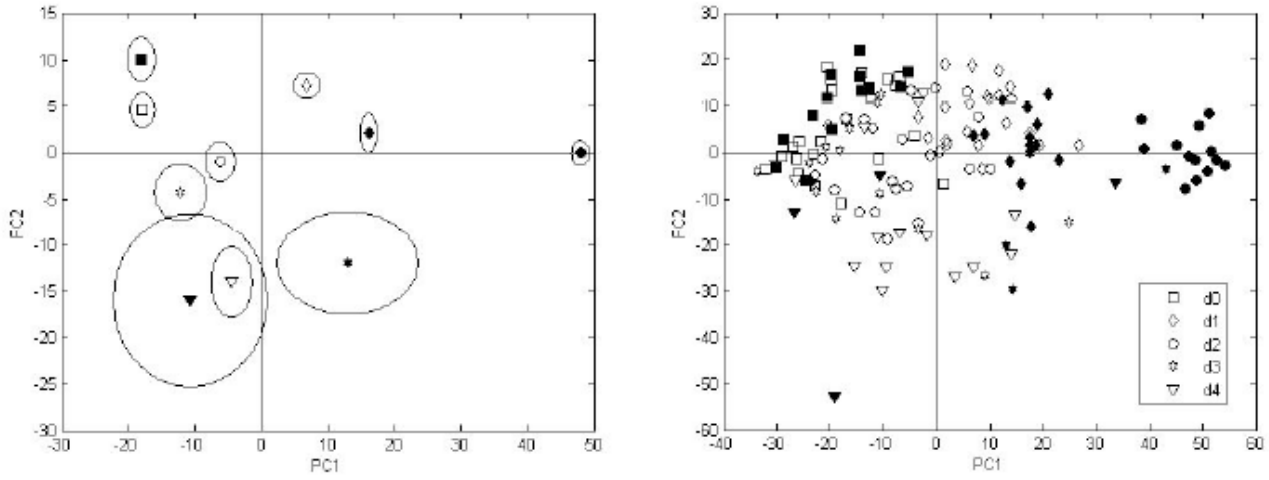

Figure 3. Representative PCA plot displaying data points for animals exposed to 50 mg/kg ANIT and controls as a function of time.

Left Panel: Data are presented as in Figure 2, where encircled data points represent mean ± SE for each group-time data. Right Panel: Data points represent PCA mapping position for all animals in ANIT treated and control groups. Sample size (n-value) at each time point is given in the legend to figure 2.

The plots in Figures 2 and 3 show differences in the mapping positions reflecting changes in biochemical composition of the urine between control and ANIT treated animals. Additionally, changes in the urinary mapping position (i.e. biochemical composition) over time were observed for the corn oil vehicle control group, presumably due to metabolism of the corn

oil. The vehicle control group mean values for day-one are separated from the day-zero (pre-dose) data, and at days two and three show a trajectory back towards pre-dose values (n=22). However, at day four the trajectory of the vehicle control again moves away from the pre-dose position. This is most clearly seen in Figures 2A-D (the scale in Fig. 2E and 2F is too large to show the dispersion in control data points).

In general, urine spectra of animals least affected by ANIT exposure mapped in the general vicinity of coordinate clusters relating to vehicle control. The two lowest dose groups (0.1 and 1 mg/kg) shown in Figures 2A and 2B, respectively, appear similar to control data at all time-points. At 10 mg/kg ANIT (Fig. 2C), the day-one and day-two data for the treated group cluster together, while the vehicle control group moves back towards the pre-dose position along PC1. Clear separation between control and ANIT treated animals, however, was observed between day-one and day-two (24 - 48 h post-dose) with doses $\geq$ 20 mg/kg (Figures 2D-F; Figure 3). Although there was some partial overlap of the day-one time point at the 20 mg/kg ANIT dose (Figure 2D), the means between the control and treatment groups are clearly separated at this time point, and this separation is greatly increased at day-two. By day-four, however, there appears to be an overlap of mapping position between vehicle control and ANIT treated animals for doses $\leq$50 mg/kg, reflecting a newly established control mapping position (Figures 2A-E and Figure 3A). The 100 mg/kg ANIT group does not exhibit this overlap at day-four indicating that differences in mapping position between control and ANIT treatment at this time point are due to ANIT exposure and not corn oil (Figure 2F).

The PCA trajectories (Figure 2) are quite informative when viewed as a function of ANIT dose and time. At 20 mg/kg, trajectories moved away from controls on days one and two, but clustered with controls again on days three and four. A similar pattern is seen for 50 and 100 mg/kg doses, but the recovery during days three and four are clearly different, as would be expected with sustained tissue toxicity. A comparison of 50 and 100 mg/kg doses shows that the former returns to control positions in the PCA plot, while the latter remains separated from controls at day-four. Indeed, clinical chemistry data showed recovery for 50 mg/kg at day-four, but plasma ALKP, AST and ALT remained elevated following exposure to 100 mg/kg ANIT

(Tables 1 and 2). Effects of ANIT at low doses (<20 mg/kg) were minimal indicating that an adaptive process is occurring without producing any overt signs of toxicity. Histopathology and clinical chemistry data corroborate this result (Tables 1, 2, and 3). The observed liver histopathology was consistent with effects known to occur in liver following exposure to the model cholestatic liver toxicant ANIT (Chisholm and Dolphin, 1996; Plaa, and Priestly, 1976). Although clinical chemistry data were not obtained on day-two for doses other than 50 mg/kg, toxic effects were evident at day-one following doses ≥50 mg/kg ANIT. These effects (elevated plasma ALT and AST) subsided by day-four following 50 mg/kg ANIT, but animals failed to recover fully by day-four at a dose of 100 mg/kg. These results were similar to those reported previously for ANIT exposures in rats (Clayton et al., 2004; Robertson et al., 2000; Beckwith-Hall et al., 1998; Chisholm and Dolphin, 1996). Correspondingly, the metabonomics urinary PCA (Figure 2) shows a separation between vehicle-control and treated at day-one for both 50 and 100 mg/kg ANIT doses, but at day-four this separation was only evident for the 100 mg/kg dose. Thus, classic plasma indices of liver toxicity and urinary metabonomics indices agree, and urinary metabonomics analyses appear to be reflective of the liver response as a function of dose and time.

Because the maximal effect of ANIT on urinary metabolites was observed at day-two post-dose in the PCA scores plots as a function of time, we constructed a dataset for all groups (treated and control) using only the day-two data and conducted a PCA. Again, the control group for this analysis included vehicle control animals from all studies grouped together (n = 22). The scores plot (PC1 *vs*. PC2) depicted in Figure 4 (Left Panel) shows a clear separation of groups in PC space as a function of dose. A plot of the mean PC1 value versus dose (0 to 100 mg/kg), as shown in Figure 4 (Right Panel), yield a good fit to a linear correlation line ($r^2 = 0.985$).

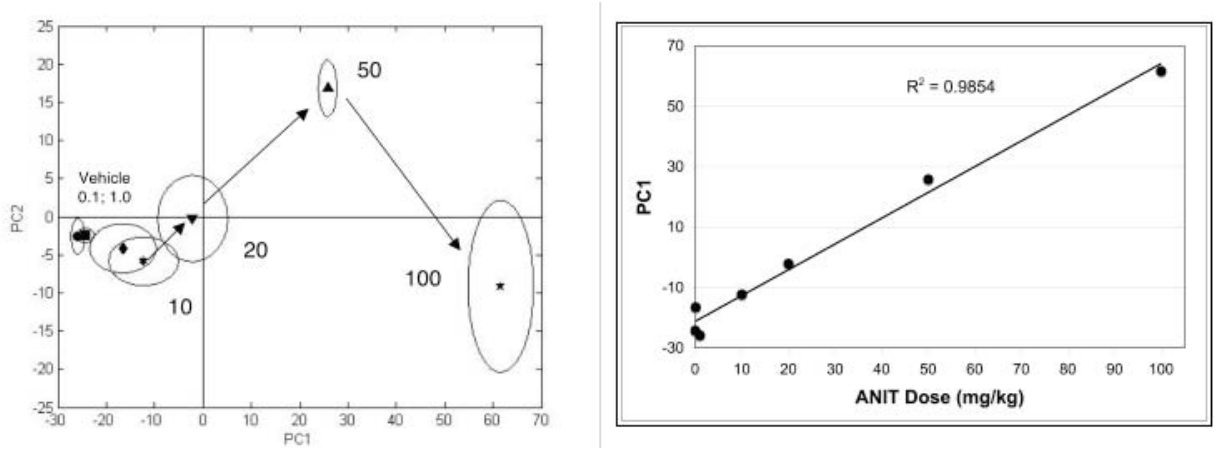

Figure 4. PCA of ANIT dose-response for urinary metabolite data measured at day-two. *Left Panel: shows the PCA scores plot (PC1 vs. PC2) for vehicle control and each ANIT dose group (0.1 to 100 mg/kg) measured at day-two. Data are presented as in Figure 2 with encircled data points representing the mean ± SE for each group (n-values are given in the legend to Fig 2). PCA vector trajectories represent ANIT-induced changes in mapping position with respect to dose (as labeled in plot). The mean PC1 value for each group plotted versus dose is shown in the Right Panel along with a linear correlation line fit (r2=0.985).*

The data plotted in PC-space (Figure 4) show a clear dose response curve for ANIT. The low doses (0.1 and 1 mg/kg) cluster very near the control group (vehicle only), but as the dose increases (10 mg/kg and above) the groups move increasingly apart from one another. Indeed, there is a strong linear correlation ($r^2 = 0.985$) between the mean PC1 value and ANIT dose (Fig. 4, Right Panel). The between-group separations are largest as doses progress from 20 to 50 to 100 mg/kg ANIT. Therefore, there seems to be a distinct transition in the range 20-50 mg/kg that corresponds with a level of severity in biological effects that leads to tissue damage. Indeed, the 50 mg/kg dose shows significant effects in clinical chemistry data at days one and two that appears to resolve by four-days post-dose (only minimal-to-mild effects in liver pathology are observed at day-four). Furthermore, no observable clinical chemistry or histopathology effects were noted at these time points for ANIT doses ≤ 20 mg/kg.

3.2.2 LDA Results.

Since doses of ≥20 mg/kg showed significant effects in urinary metabolite profiles as determined by PCA analysis, we conducted LDA and hierarchical clustering analysis at these doses (Figures 5 and 6) to examine further the spectral features that account for these effects. Interestingly, the data clearly show significant changes in the urinary metabolite profiles at doses ≥20 mg/kg ANIT that revealed similar patterns suggesting a characteristic toxic effect of ANIT exposure. Furthermore, these data also demonstrated a unique change occurring at 100 mg/kg.

Overall, the maximal dose-response effect of ANIT as determined from the urinary metabolite PCA trajectories (Figures 2 and 3) occurred at two-days post-exposure. Therefore, we conducted a LDA for each dose group versus vehicle control at the identical day-two time point. Two-dimensional plots of the first two LD projections for each dose group versus controls showed separation for doses ≥20 mg/kg, but only the 50 and 100 mg/kg doses produced a clear "within group" clustering of treated samples and control samples with a complete separation between groups (Figure 5). The LDA coefficients of the first discrimant vector (LD1) provided a ranking of bins (most significant to least significant) for the 20, 50, and 100 mg/kg groups vs. controls.

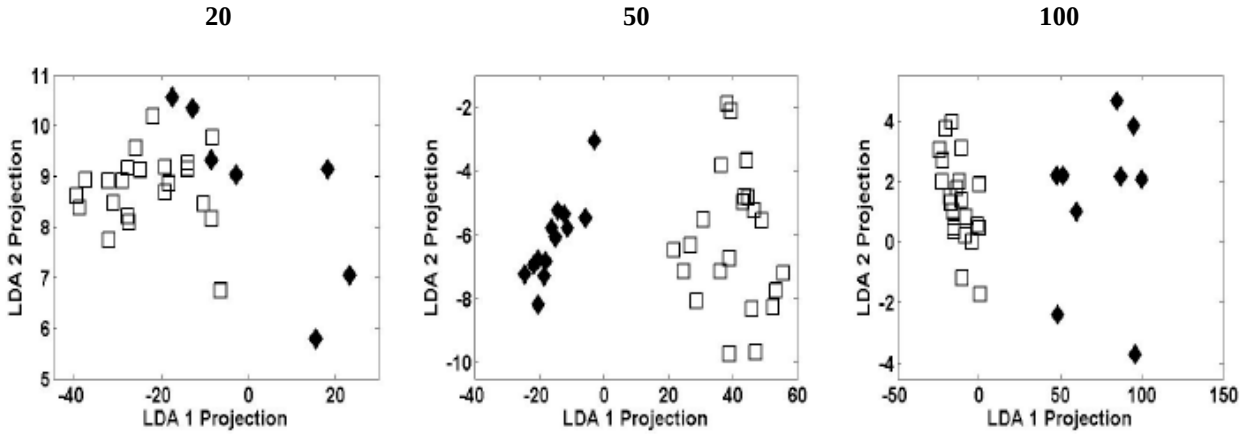

Figure 5: Linear Discriminant Analysis (LDA) for 20, 50 and 100 mg/kg ANIT dose groups (filled diamonds) versus vehicle-treated controls (open squares) at two-days post-dose. *The plots (LDAprojection 1 vs. LDA projection 2) show the clustering of samples within groups and separation between groups, particularly for the 50 and 100 mg/kg doses. Note that the scale of the axes also increases with increasing dose indicating greater discrimination of group clusters.*

We then took the absolute value of the LDA coefficients normalized across each dose group and compiled a list of bins from the top 50% by LDA weight from each of the three dose groups. The combined list from all three dose-groups yielded a total of 31 unique bins, which were then compiled with their associated weighting factors and used as input for a hierarchical clustering analysis by the centroid method (JMP software, SAS, Inc.). Figure 6 shows the dendrogram and color heat-map from this analysis in which a two-way clustering was conducted for salient bins (listed by chemical shift values, ppm, at the bin center) versus ANIT dose (20, 50, and 100 mg/kg). Two observations are noteworthy: 1) there is a set of bins (spectral regions) with similar significance across all doses, and 2) the 100 mg/kg dose shows a few bins that are uniquely different than the lower doses. With regard to the former observation, the top portion of the color map in Figure 6 shows 13 bins with about equal significance across all doses (gray/blue), and the bottom portion of the figure contains 5 bins that are also similar across dose but of greater significance (red). These are predominately signals from citrate, α-ketoglutarate (2-oxo-glutarate), and trimethylamine oxide (TMAO; presumably betaine), which are known to decrease significantly in urine following ANIT treatment (Waters et al., 2002; Waters et al., 2001).

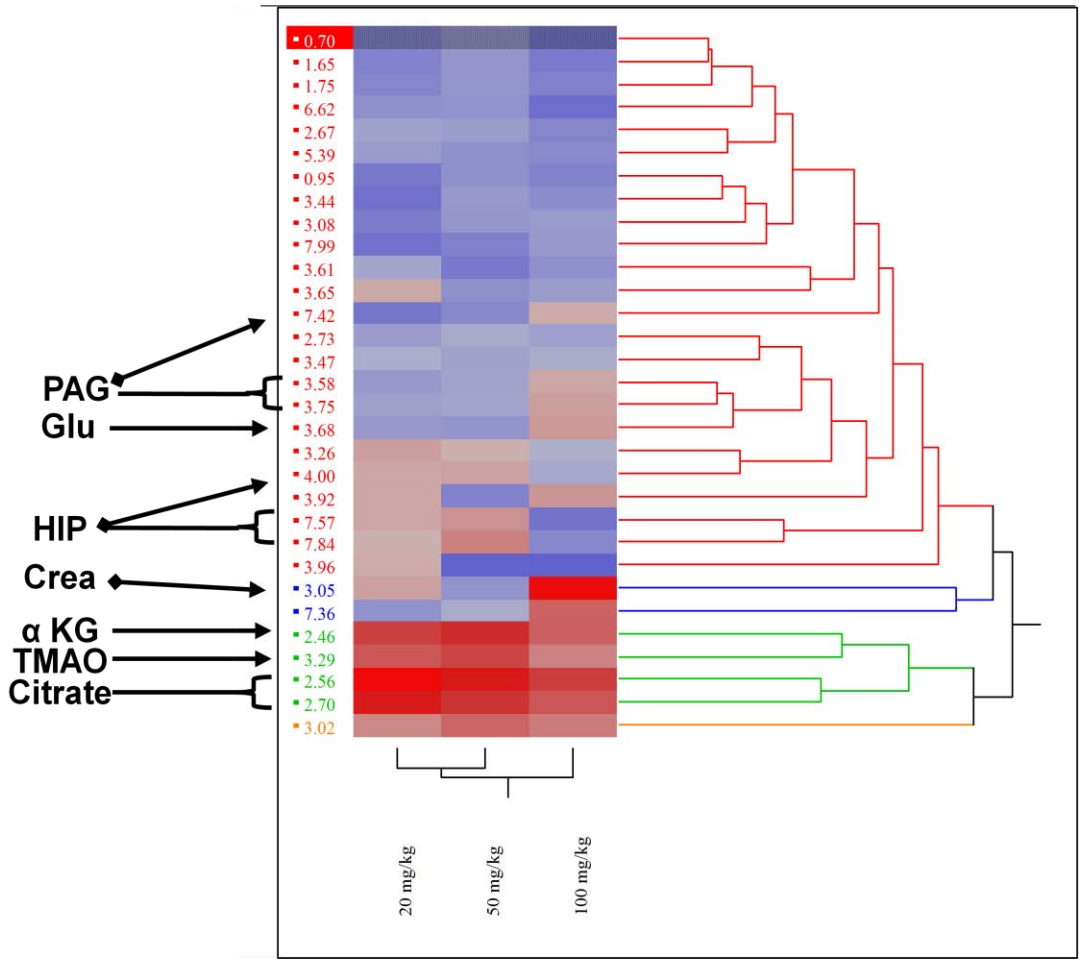

Figure 6: A hierarchical clustering analysis for the 20, 50, and 100 mg/kg ANIT dose groups.

The dendrogram and color map depicts 31 bins labeled along the left edge as the chemical shift (ppm), and the columns represent each ANIT dose (labeled at the bottom of the map). The bins or ppm are grouped according to similar patterns in the weighting factors (LDA coefficients). Metabolite abbreviations corresponding to ppm(s) indicated at left are: phenylacetylglycine (PAG); hippurate (HIP); glucose (Glu); creatine (Crea); alpha-ketoglutarate (αKG); and trimethylamine oxide (TMAO). The data show sets of spectral features that define high dose, particularly 100 mg/kg versus the two lower doses (see text for details).

Additionally, there is a change in the metabolite profile, particularly for the 100 mg/kg dose in comparison to 20 and 50 mg/kg. At 100 mg/kg it appears that signals at 7.42, 3.58, 3.75, 3.68, 7.36, and 3.05 ppm show increased importance (in the order listed). Three of these signals (3.75, 7.36, and 7.42 ppm) are all assigned to phenylacetylglycine (PAG), the signal at 3.05 ppm is from creatine, the signal at 3.68 ppm is glucose and the signal at 3.58 is unknown. Both PAG and creatine show increased urinary excretion at day-two post-dose with 100 mg/kg ANIT, which is a distinguishing feature for this dose versus lower doses.

An interesting observation is illustrated in the cluster analysis for 20, 50, and 100 mg/kg doses (Figure 6). The urinary profiles show subtle changes in metabolites across this dose-range, but these are easily discernible in the PCA scores plots (Figures 2 and 4). The similar effects of ANIT across dose include a decrease in urinary excretion of citrate, hippurate, α-ketoglutarate (or 2-oxo-glutarate), and TMAO. Slight changes in the relative amounts of these compounds likely account for much of the differences between ANIT doses up to about 50 mg/kg; recovery from these ANIT doses (at times beyond day-two) is evident in the PCA trajectories (Figure 2) and the blood clinical chemistry data (Table 1). Unique features evident only at the highest ANIT dose are also revealed by this analysis. One unique feature is the level of urinary creatine, which was elevated at 100 mg/kg ANIT exposure and represents the most important spectral feature (signal at 3.05 ppm) that separates treatment from control at day-two post-dose. Additionally, changes in PAG and hippurate are important discriminating factors, whereby ANIT caused an increase in urinary PAG and a decrease in hippurate (Figure 1). However, at 100 mg/kg ANIT the level of significance for PAG (7.42, 7.36 and 3.75 ppm) was greater than it was at 20 or 50 mg/kg, while hippurate (4.00, 7.57 and 7.84 ppm) showed the opposite trend of being a more important factor at the lower doses. Thus, these three metabolites (creatine, PAG, and hippurate) provide discriminating features for doses from 20 – 100 mg/kg ANIT. The changes observed for citrate and α-ketoglutarate (decreased excretion relative to controls) are important features of ANIT toxicity, but they do not provide discriminatory information about the dose-dependent effects within the range from 20 – 100 mg/kg (Figure 6). This type of information would not have been obtainable without this time- and dose-response analysis. The more severe effects of ANIT toxicity are clearly evident at 100 mg/kg, where creatine and PAG urinary excretion

increases, blood chemistry shows elevated liver enzymes, and marked effects are noted in liver pathology. Others have also noted profound effects of 100 mg/kg ANIT in rats including urinary excretion of bile acids (Uchida et al., 2002; Waters et al., 2002; Waters et al., 2001; Chisholm and Dolphin, 1996) and elevated urinary creatine (Clayton et al., 2004; Robertson et al., 2000; Waters et al., 2001; Beckwith-Hall et al., 1998), as seen herein. Additionally, the elevation of plasma enzymes indicative of liver damage was observed at both day-one and day-four post-dose at 100 mg/kg ANIT (Table 1), which corroborates studies by others using this same dose (Clayton et al., 2004; Robertson et al., 2000; Beckwith-Hall et al., 1998; Chisholm and Dolphin, 1996). These techniques can pave the way for the detection of both biomarkers of exposure, which typically occur at low doses, as well as biomarkers of toxicity that occur at higher doses. It is clear that following a single low dose exposure to ANIT (≤10 mg/kg) maximum effect and recovery occur within four days post-dose, and this chemical exposure can be monitored by PCA of urinary metabolite profiles. At higher doses, the urinary metabolite patterns indicate that exposure and toxicity are both evident (particularly above ~20 mg/kg), recovery is not complete by day-four, and such results correlate with established toxicity assays. The biochemical basis for these metabolic effects is presumably related to a disruption of mitochondrial energy metabolism in exposed animals since the levels of citric acid cycle intermediates (citrate and α-ketoglutarate) decreased. Glycine metabolism may have also been impacted since the levels of urinary excretion of hippurate (benzoylglycine) and PAG were affected by ANIT treatment. However, changes in the level of these two metabolites more likely reflects the effects of ANIT on gut microflora (Nicholson et al., 2005). Furthrmore, at 100 mg/kg ANIT exposure, the urinary excretion of creatine in F344 rats was increased, which is interesting since liver does not contain creatine kinase activity; however, creatine is synthesized in the rat liver by methylation of guanidoacetate via guanidoacetate methyltransferase (Loo et al., 1986). Elevated urinary creatine following ANIT exposure has also been documented in other strains of rats such as Wistar (Waters et al., 2001; Robertson et al., 2000) and Sprague-Dawley (Clayton et al., 2004; Beckwith-Hall et al., 1998). This dose of ANIT may also be impacting other tissues in addition to liver (i.e. heart and muscle), or biosynthetic pathways in the liver. Others have demonstrated similar effects of ANIT on tissue metabolism including effects on citric acid intermediates and decreased bile acid production (Shockcor and Holmes, 2002).

3.2.3 Spectrum Profiling: Application of Chenomx NMR Profiler.

In order to identify important metabolites and possible biomarkers, the Chenomx NMR Profiler application was initially applied to one sample selected from the controls and one sample selected from the ANIT treatment group. These samples were chosen based on their large degree of separation in the PLS-DA scores plot (Figure 7). Two additional samples (control and ANIT treated) were then profiled in order to assess whether the qualitative conclusions drawn from examining the first pair are also exhibited in the second pair. It was observed that both pair-wise analyses were consistent, and therefore the spectra of these samples were annotated in detail.

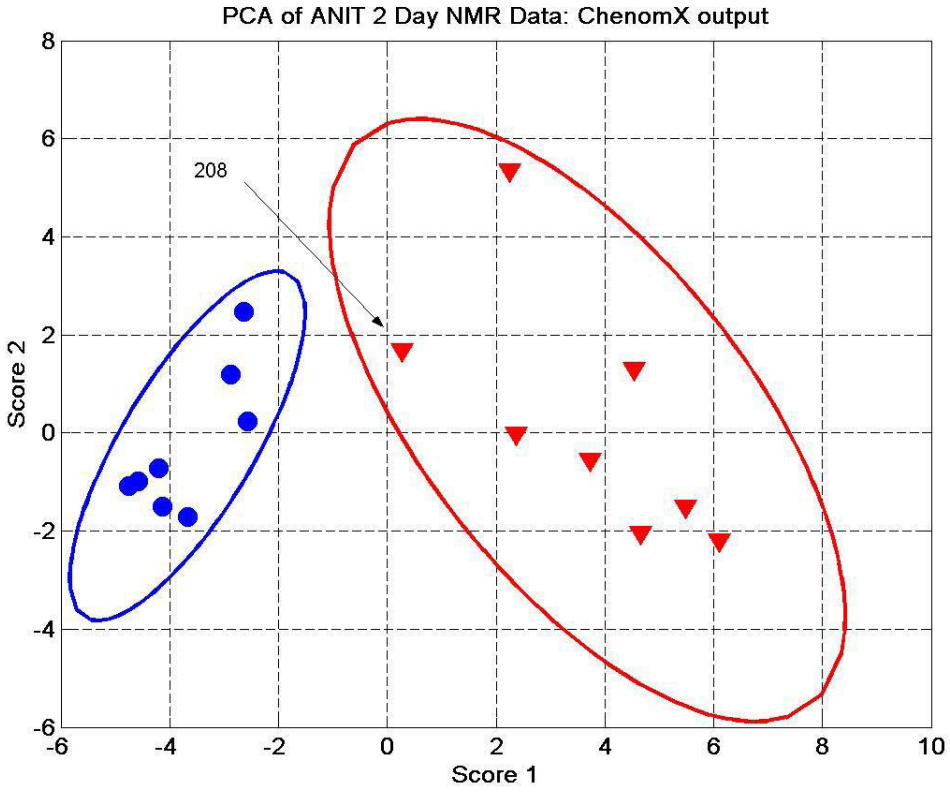

Figure 7: Scores plot of Pareto scaled, Chenomx software processed, 0.04 ppm binned, normalized spectra of the 48 hour post-dose ANIT data. Blue discs are controls.

Red triangles are 50 mg/kg dosed subjects.

In the figure above, Sample 208 is identified because it was decided to delete it in the subsequent PLS-DA analysis. This decision was made because it slightly improved the percent variation captured in the first PLS-DA component, and it was assumed that this fact would lead to a more clearly interpretable PLS loading analysis. However, it is believed that the impact of deleting Sample 208 is minor and that all of the subsequent results would also follow from an analysis that includes Sample 208.

We noted that metabolite concentrations needed to be adjusted by a normalization process prior to making comparisons between controls and ANIT-dosed samples. A simple way to normalize can result from dividing all sample concentrations by the creatinine level of the corresponding samples. By implementing this procedure, comparing the four spectra in detail, by examining the loadings in detail and by studying the research literature, at least 19 metabolites were identified that warranted further detailed investigation (Table 4).

Table 4: List of potentially interesting metabolites resulting from the 48 hour ANIT (50 mg/kg) analysis. This list is preliminary and not comprehensive.

1-Methylnicotinamide	Formate	Oxalacetate
2-Oxoglutarate	Fumarate	Phenylacetylglycine
Acetate	Glucose	Succinate
Acetoacetate	Hippurate	Trigonelline
Betaine	Mannose	Trimethylamine N-oxide
Cholate	NAD+	trans-Aconitate
Citrate		

The above Table is only preliminary, and further investigation is being conducted. However, it should be noted that some of the metabolites (e.g. trigonelline and NAD+), might not have been discussed in the prior published literature on ANIT toxicity and metabonomics.

Known biomarkers of ANIT exposure identified in the literature using NMR (Shockcor and Holmes, 2002), as well as those identified by NMR in the present study using hierarchical clustering analysis and Chenomx NMR Profiler software described above, include: acetate, bile acids, glucose (up-regulated); citrate, hippurate, 2-OG, and succinate (down-regulated). Consistent across all ANIT dose levels ≥10 mg/kg was the observation of a decrease in urinary excretion of citrate, α-ketoglutarate, trimethylamine oxide (TMAO; an oxidation byproduct of choline and dietary methylamines), and hippurate. Others have also reported decreased excretion of citrate, succinate, α-ketoglutarate, and hippurate in NMR-based metabonomics studies of ANIT toxicity in the rat (Waters et al., 2002; Waters et al., 2001; Robertson et al., 2000; Beckwith-Hall et al., 1998). Our observation of decreased TMAO excretion, however, does not appear to be a major finding in these other reports. In fact, Waters, *et al*. (2001) found an increase in urinary excretion of TMAO at 144 h post-dose with 150 mg/kg ANIT in Han-Wistar rats. Thus, the metabolism associated with methylamines may be strain/species dependent and, consequently, not a useful biomarker of cholestatic hepatotoxicity.

3.3 UPLC/MS Analysis (Negative-Mode) of Urine Samples (Solutions Labs, Cambridge, MA)

The negative mode data using above UPLC-MS conditions yielded excellent group separation (Figure 8). After cleaning the data set using the previously described filtering, an automated metabolite identification was run and several interesting metabolites (e.g. glycocholate and taurocholate) were highly ranked, but no retention time (RT) library existed for these solvent conditions. As a result, identifications were inconclusive at present.

The second set of negative mode acquisitions utilized the same solvents as positive mode studies. Unfortunately, the resulting data set yielded over 180 ion species whose intensities were saturated. Because of the highly skewed distribution (typical of UPLC-MS data in general) of ion intensities across all the species (large fraction of total sample intensity coming from a small

fraction of metabolites), we believe that this data set is of insufficient quality to analyze. Since the saturation for these solvent conditions was most likely caused by insufficient dilution, we doubled the dilution to 6:1 in a planned follow-up study.

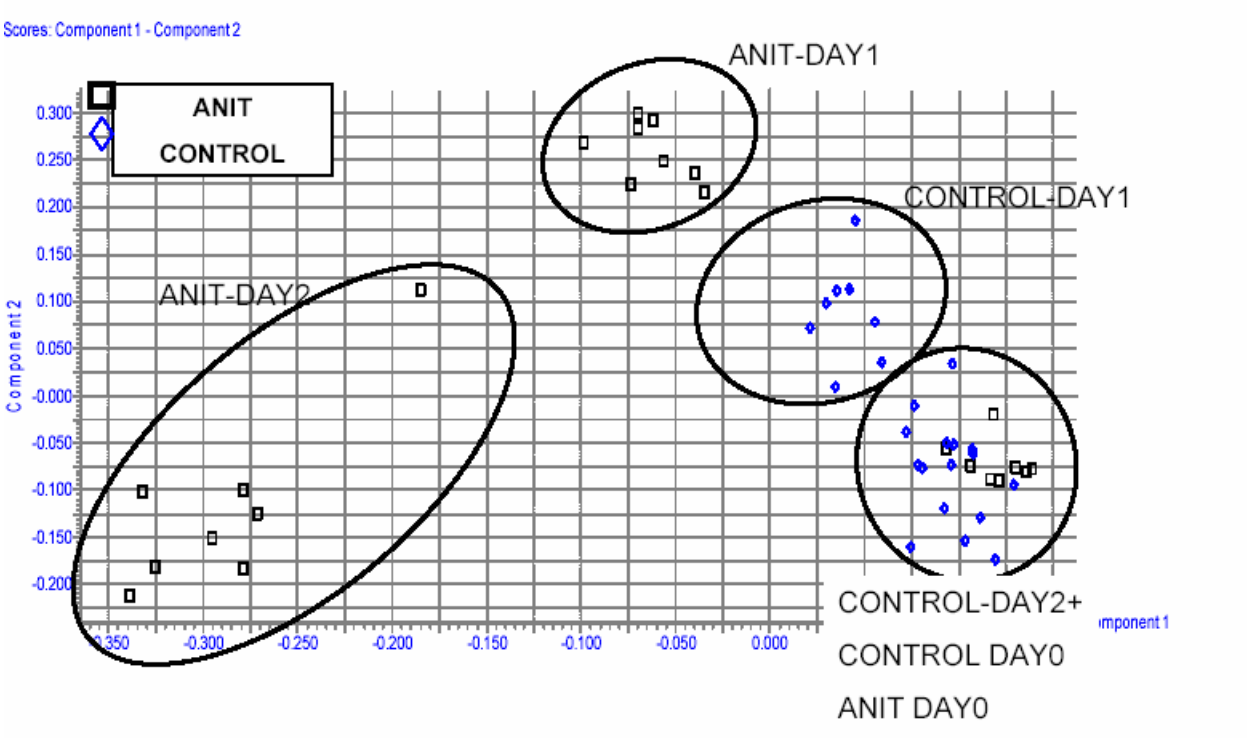

Figure 8: PCA plot of Markerlynx mean centered, UV scaled negative ion mode data (15,000 variables) for Ammonium Acetate in the solvents.

3.3.1 UPLC/MS Analysis (Positive-Mode) of Urine (Solutions Labs, Cambridge, MA).

Previous analysis attempted to extract markers from a two-sample group comparison of controls and ANIT dose group at day-two, since the maximum perturbation of the metabolic

profile occurred at the second day. However, PCA analysis of the full UPLC/MS data set clearly shows that samples of the ANIT dosed animals from the first day cluster coherently away from both controls and the second day samples. Thus, it would be possible to conduct a comprehensive analysis of the day-one data that corresponds to that attempted with the day-two data. Results derived from day one analysis would yield markers not present at day-two and vice versa due to the time dependent nature of perturbations to the metabolic profile. Rather than identifying differences between types of markers present in the samples of day-one and day-two, it was decided to identify markers that exhibit strong differential regulation in the day-one data that also either maintain a similar level of differential regulation at day-two or show an increased/decreased trend in the same direction. The motivation for this analysis was the discovery of markers for early detection of a pathological process. Moreover, it was conjectured that at least some of these markers might persist in the data collected beyond day-two. If this hypothesis is correct, then these particular types of markers might be strong candidates, subject to establishing their biological specificity, for inclusion in a toxicity exposure detection system.

Four two-group PLS-DA analyses (two for each day) were conducted in order to rank variables. They included: (i) day-one controls versus day-one 50mg/kg ANIT using a data matrix normalized using the total sum of intensities for each sample; (ii) day-one controls versus day-one 50mg/kg ANIT using a data matrix normalized using the total sum of intensities for each sample. This normalization was followed by a logarithmic transformation of the data; (iii) and (iv): the day-two analysis corresponding to (i) and (ii). After normalization (and logarithmic transform in cases (ii) and (iv), the data matrix was processed with a unit variance scaling across each variable (i.e. intensities of each m/Z and RT combination).

The analyses with logarithmic transformation were considered due to theoretical studies in the literature with regard to advocating the use of these transformations due to their ability to effect variance stabilization. However, our experience indicated that while log transformed data often uncovers interesting features (i.e. high ranked variables), it appears to be over-sensitive to outliers in some variables. We have found in prior research that analyses without log transformation should also be conducted and compared to the transformed data.

After concluding the variable ranking, a procedure was implemented in order to tentatively identify candidates for early onset biomarkers. The rankings and two data matrices (day-one and day-two) were used to select variables with the following properties: (i) for each day, the highest of the two rankings should be less than 150; (ii) for each day, the lowest of the two rankings should be less than 800; (iii) variables meeting the first two specifications should also have mean intensities in the upper 25% of readings in their respective data matrices. The last requirement follows from the assumption that variables with a strong signal are compounds that might be in high enough concentration to be detectable by methods other than mass spectrometry. Although this procedure needs to be subjected to further testing and refinement in order to define the optimal constraints for variable selection (e.g. perhaps lower intensity variables should also be considered), we have already found interesting candidate variables for further study.

A list of 19 variables was selected by the above procedure. To illustrate the potential value of these results, an example of a normalized trends plot of one selected variable (m/Z = 448.1048 and RT = 5.073) is presented in Figure 9. We believe that it should be possible to extract early onset markers from the UPLC-MS profile data if the actual chemical identity of candidate biomarkers may be found in order to assess biological specificity.

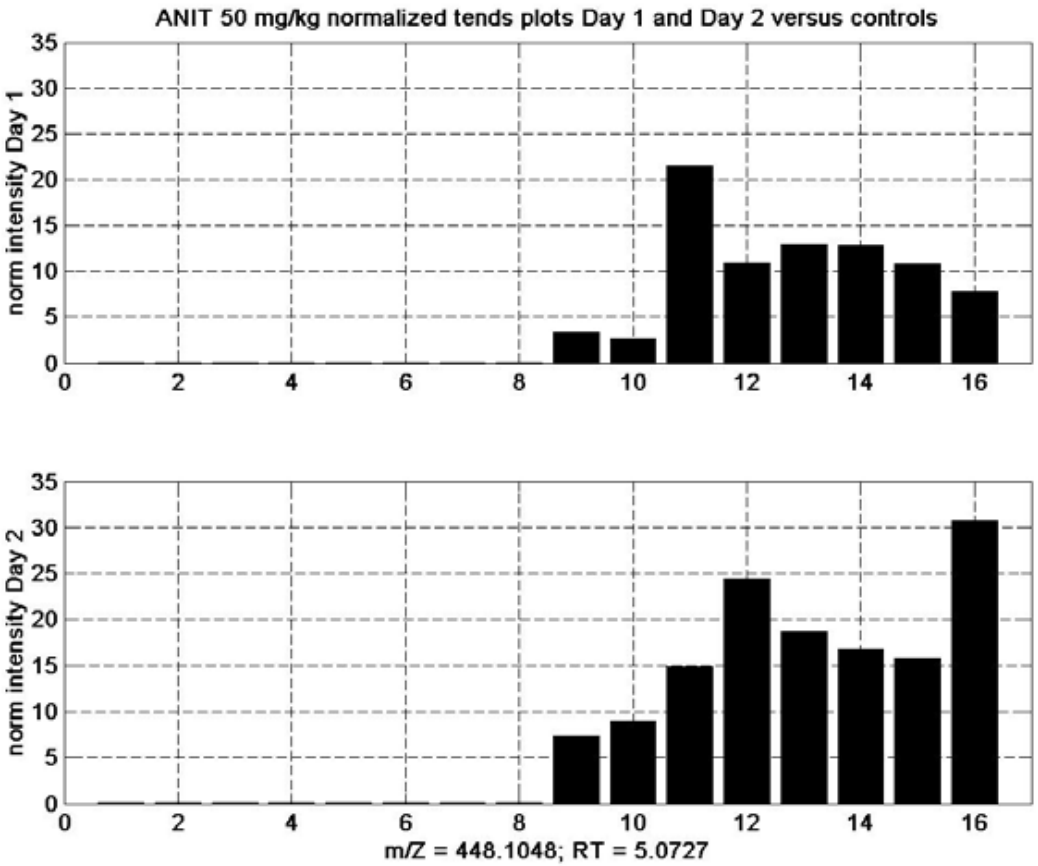

Figure 9: Normalized ion intensity across samples for ion species with m/Z = 448.1048 and RT = 5.073.

Top panel is data from day one and bottom panel is day two data. First 8 subjects are control animals and subjects 9 to 16 are animals dosed with 50 mg/kg of ANIT.

3.3.2 PCA Analysis of High-Dose ANIT Data (Solutions Labs, Cambridge, MA).

Positive ionization mode UPLC-MS data for the high-dose ANIT (100 mg/kg) was acquired as described above with the exception that mass scanning was restricted to masses up to 850 Daltons. After processing the centroid mode data with Waters MarkerLynx software, the de-isotoped output data matrix consisted of approximately 22,000 variables. In order to eliminate non-informative variables, we applied two filtering procedures to create two separate data sets

that were individually analyzed. The first filtering procedure is an "endogenous metabolite filtering" that is implemented by demanding that a variable have a non-zero reading in at most three animal subjects at the pre-dose time of zero hours. This filtering results in approximately 1600 variables being retained in the data matrix. The second filtering scans through variables that were eliminated by the first filtering, and it adds variables back into the data if the variables have at most two non-zero readings in the samples corresponding to high-dose maximum response (i.e. 48 hours). This filtering leads to a data matrix of about 3200 variables. Some of these variables will be xenobiotics, but others will be endogenous metabolites that are below the detection limit in animal subjects not perturbed by ANIT. After further manipulation of the data, involving sum normalization, logarithmic transformation and unit-variance scaling, we conducted a PCA analysis to assess cluster separation and the effective dimensionality of the data. For both types of filtering, we found that the majority of the variance was contained in the first two components (Figures 10 and 11).

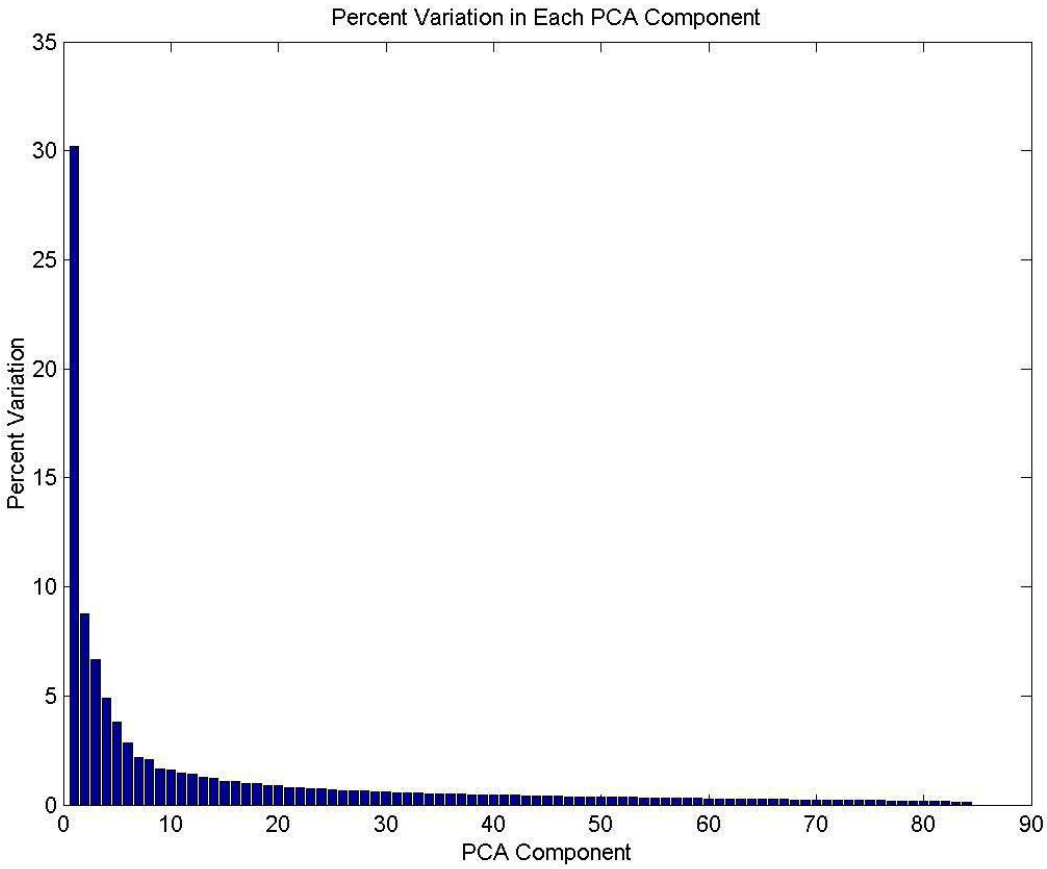

Figure 10: Percent variation by PCA component for unit-variance scaled data matrix resulting from filtering to retain mostly endogenous compounds (approx. 1600 variables).

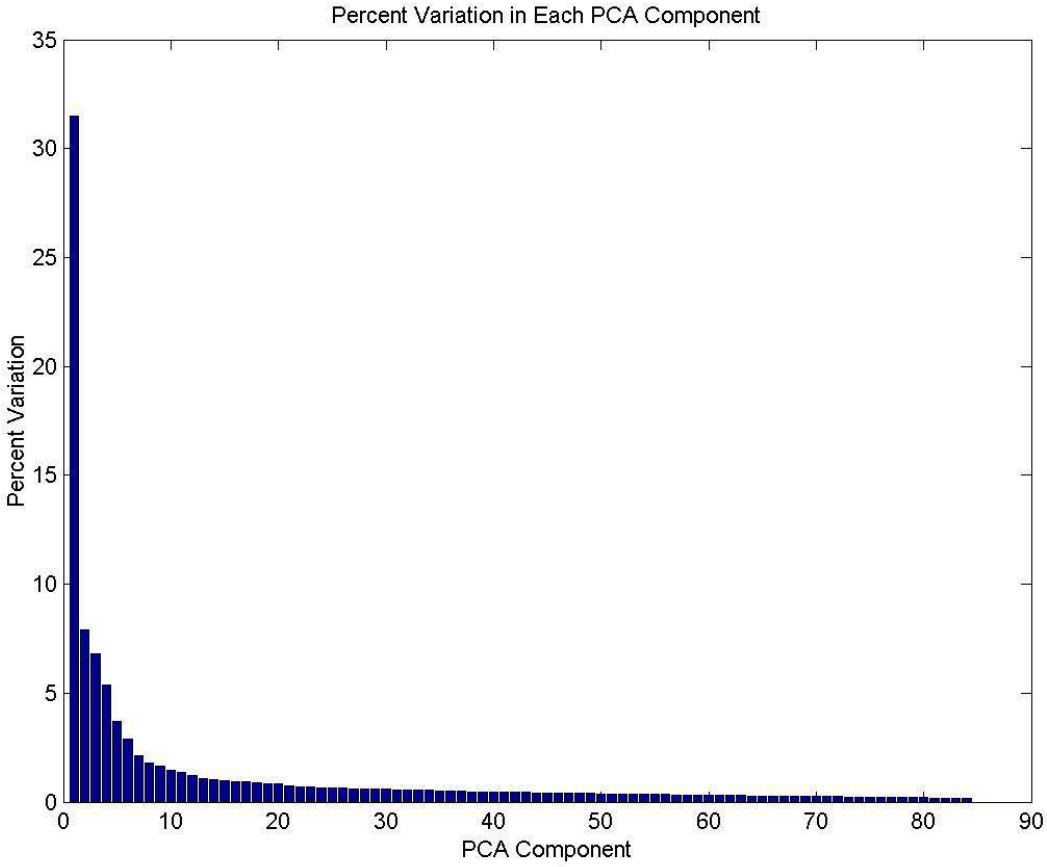

Figure 11: Percent variation by PCA component for unit-variance scaled data matrix resulting from filtering to retain mostly endogenous compounds and additional high-dose markers (approx. 3200 variables).

3.3.2.1 PCA Scores Plots (Solutions Labs, Cambridge, MA).

Scores plots were examined to identify clustering and to confirm that the first PCA component is mostly associated with ANIT exposure as opposed to normal metabolic variation between animal subjects. The 3200 variable filtering leads to better separation, and this observation is to be expected based on the strong presence of xenobiotics and of products from

bile acid synthesis that might be below normal detection (Figure 12). These compounds are expected to help induce clustering. However, the 1600 variable filtering also shows clear clustering (Figure 13), and it has another special feature. Specifically, the controls appear to drift along the second component, and if this component is assigned to individual variation and the "corn oil effect", then it can be argued that these effects are very small compared to the ANIT perturbation by noting that the first component captures much more variance than the second component (see Figure 10).

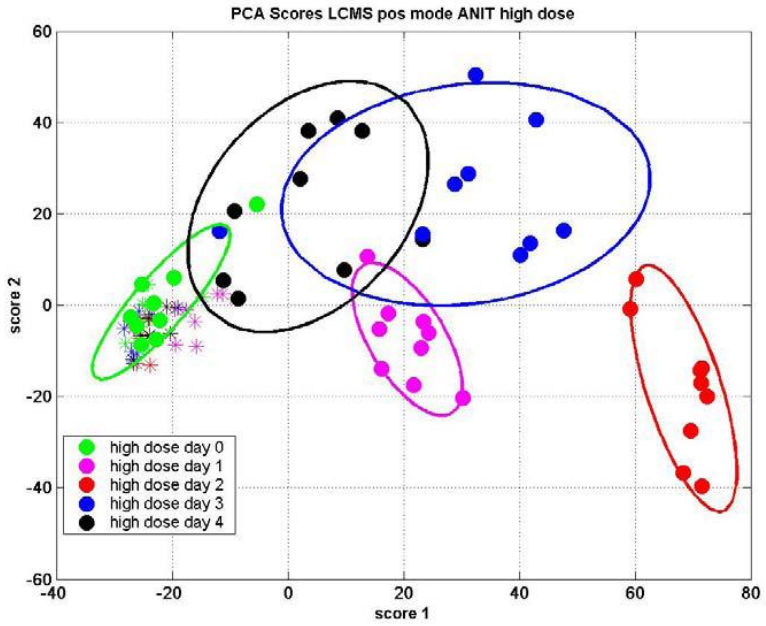

Figure 12: PCA scores for unit-variance scaled data matrix resulting from filtering to retain mostly endogenous compounds and additional high-dose markers (approx. 3200 variables). *The points plotted as stars are the control subjects at the color coded times corresponding to the dosed subject (solid dots).*

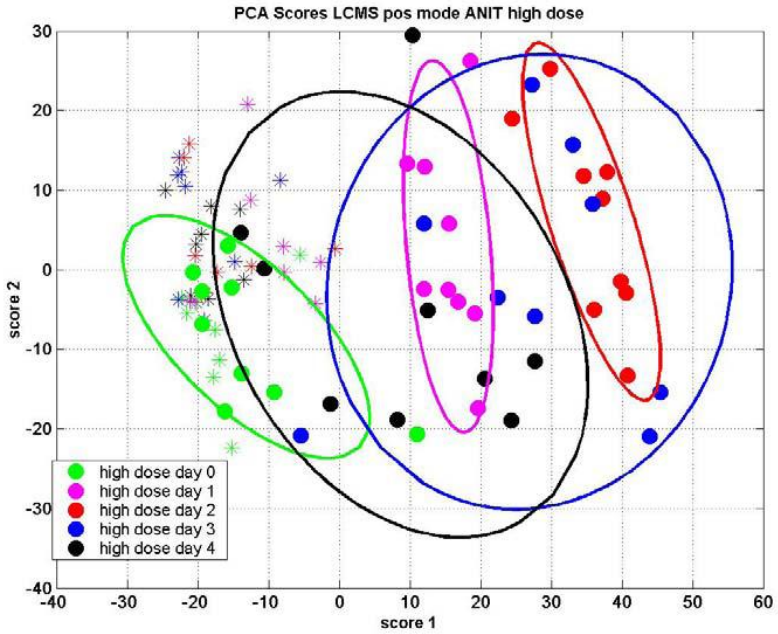

Figure 13: PCA scores for unit-variance scaled data matrix resulting from filtering to retain mostly endogenous compounds (approx. 1600 variables).
The points plotted as stars are the control subjects at the color coded times corresponding to the dosed subjects (solid dots).

3.3.3 PLS-DA and Variable Selection (Solutions Labs, Cambridge, MA).

In order to assess the importance of variables with respect to being markers for ANIT exposure (and candidate biomarkers), a subset of the data corresponding to the maximum metabolic perturbation was selected (i.e. 100 mg/kg group at two days post-dose) and compared to the controls. As usual, PLS-DA is a convenient method for ranking variables. When PLS-DA was applied to the 3200 variable data set, a clear separation of the data occurs with about 99% Y-Block variance and about 52% X-Block variance was captured by just the first component.

After completing the PLS-DA analysis, further analysis included scanning the data matrix to identify possible sodium, potassium, and ammonium adducts for each variable. This procedure was followed by looking into a 20 ppm window around each variable mass (assuming an M +

proton ionization) and comparing to the KEGG database. Over 4000 possible mappings between KEGG compounds and the data matrix resulted from the analysis, but most were false identifications. Further efforts to identify candidate metabolites were made using Solutions Labs' metabolite library, and following possible identifications were made (Table 5).

Table 5. Tentative Metabolite Identification in rat urine using UPLC/MS and PLS-DA Analysis.

Name	RT	RT library	mass exact	mass measured	mass diff	pls rank(log)
Creatine	0.714	0.74	131.0695	131.0695	0.0000	362
Betaine	0.653	0.67	117.0790	117.0793	0.0003	488
Histidine	0.821	0.61	155.0695	155.0686	0.0009	498
Citrate	1.240	1.20	192.0270	192.0272	0.0002	615
Phenylalanine	2.508	2.50	165.0790	165.0789	0.0001	643
Thiamin	0.723	0.67	264.1050	264.1012	0.0038	645
Tryptophan	3.248	3.11	204.0899	204.0892	0.0007	750
Leucine	2.030	1.98	131.0946	131.0944	0.0002	1133
Creatinine	0.696	0.67	113.0589	113.0593	0.0004	1173
4-Guanidinobutanoate	1.071	1.11	145.0851	145.0849	0.0002	1225
5-Oxoproline	1.453	1.56	129.0426	129.0427	0.0001	1240
5-Hydroxytryptophan	2.164	2.15	220.0848	220.0845	0.0003	1543
Hypoxanthine	1.255	1.22	136.0385	136.0376	0.0009	1638
Lysine	0.806	0.59	146.1055	146.1073	0.0018	1883
AMP	0.678	0.88	347.0630	347.0646	0.0016	2128
Threonine	0.784	0.67	119.0582	119.0589	0.0007	2198
Adenosine	2.068	1.99	267.0968	267.0978	0.0010	2605
Serine	0.881	0.64	105.0426	105.0432	0.0006	3054

It is noted that these metabolites are only possible identifications. However, due to high intensities of candidate metabolites (assuming a correlation between intensity and concentration) there is great confidence in their identity because these tend not to be merely artifacts from the MarkerLynx processing. To illustrate the problematic nature of UPLC-MS variable intensities, a histogram of mean variable intensities is presented in Figure 14.

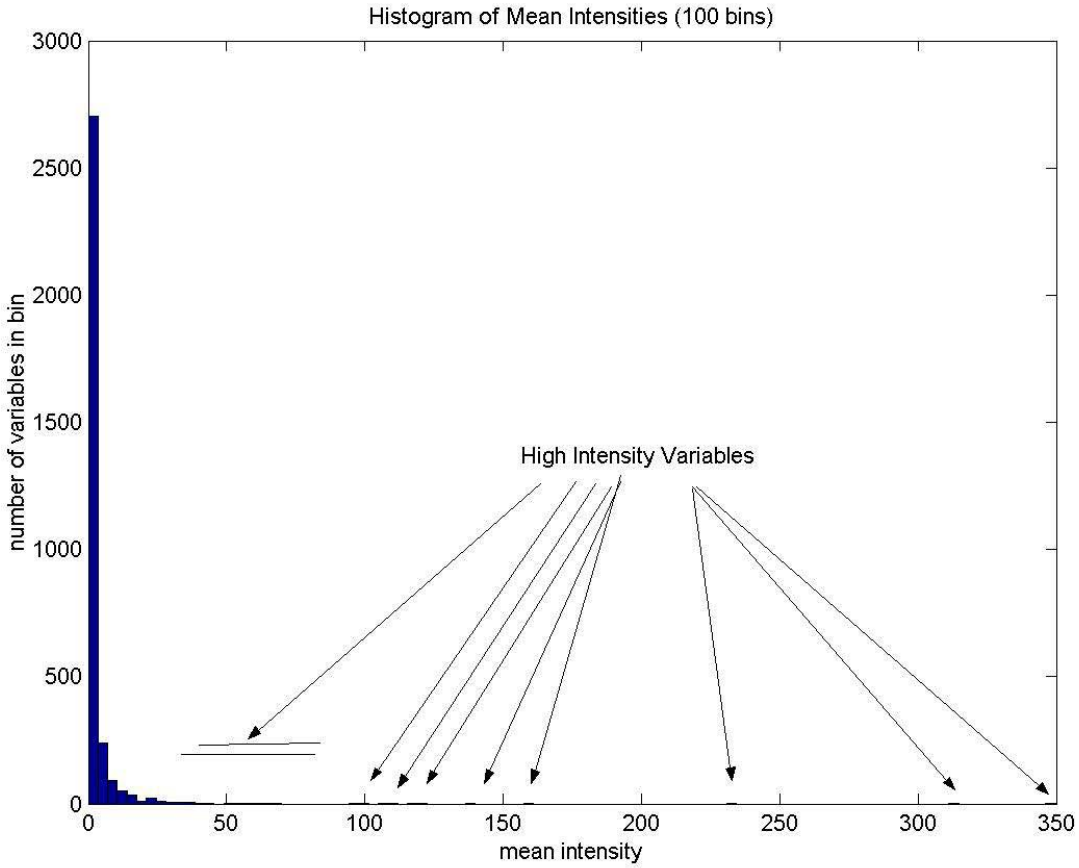

Figure 14: Histogram of normalized mean variable intensities for the 3200 variable data set. *Single outlying g variables, which are difficult to see in the figure, are indicated by arrows to make them easier to identify.*

This highly skewed intensity distribution has a mean intensity of 3.1 and a median of 0.8, and many variables are of extremely low intensities. Some of these variables are artifacts; for example, we have found one variable that has predominantly non-zero readings across pre-dose animal subjects (and hence is included in the data matrix), but it has zero readings across the reduced data matrix consisting of samples taken at 48 hours. We believe that this problem might be due to instrumental drift, and Solution Labs is developing algorithms to identify these

problems. It should be noted that these problems are very rare and seem to only exist for very low intensity variables. Therefore, it is possible to proceed with extracting useful information from current analyses as long as awareness of potential complications is noted. Ultimately, it will be necessary to go back to individual sample chromatograms to verify results found by statistical manipulation of the mass tables.

To further support the validity of a metabolite variable, it is helpful if that variable has possible adducts, since this possibility provides some additional support to the assumption that each variable has ionized via a mass plus proton mechanism when we conducted the KEGG search. Normalized expression levels of candidate metabolite markers identified across 48 hour rat urine samples is presented below (Figure 15).

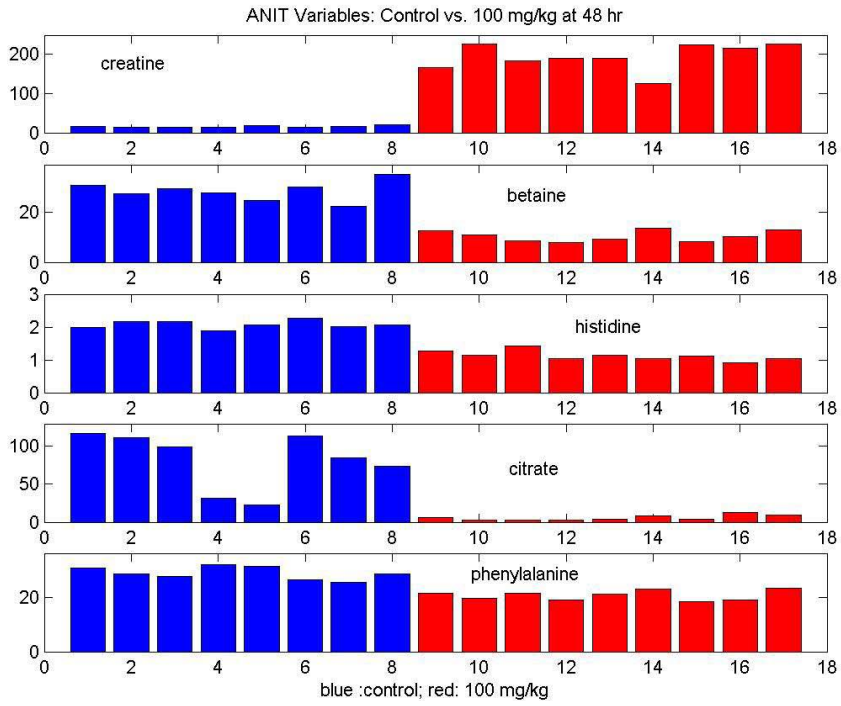

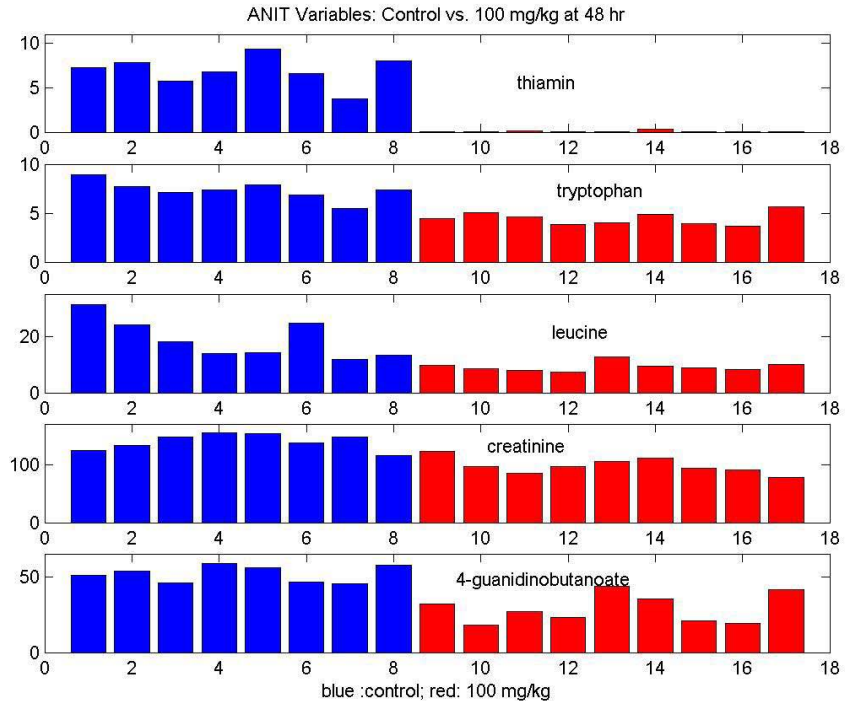
ANIT Variables: Control vs. 100 mg/kg at 48 hr
thiamin
tryptophan
leucine
creatinine
4-guanidinobutanoate
blue :control; red: 100 mg/kg

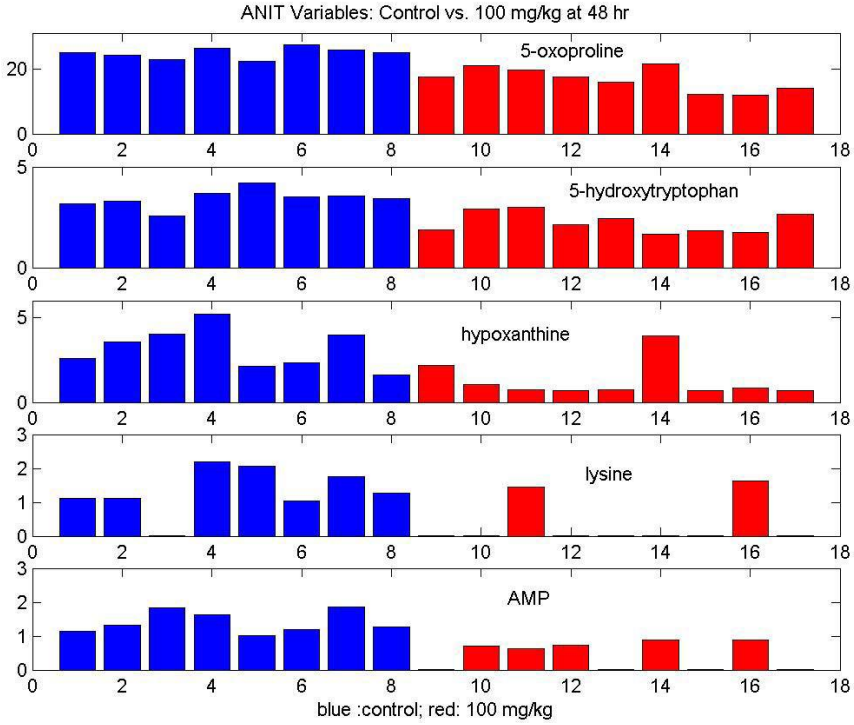
ANIT Variables: Control vs. 100 mg/kg at 48 hr
5-oxoproline
5-hydroxytryptophan
hypoxanthine
lysine
AMP
blue :control; red: 100 mg/kg

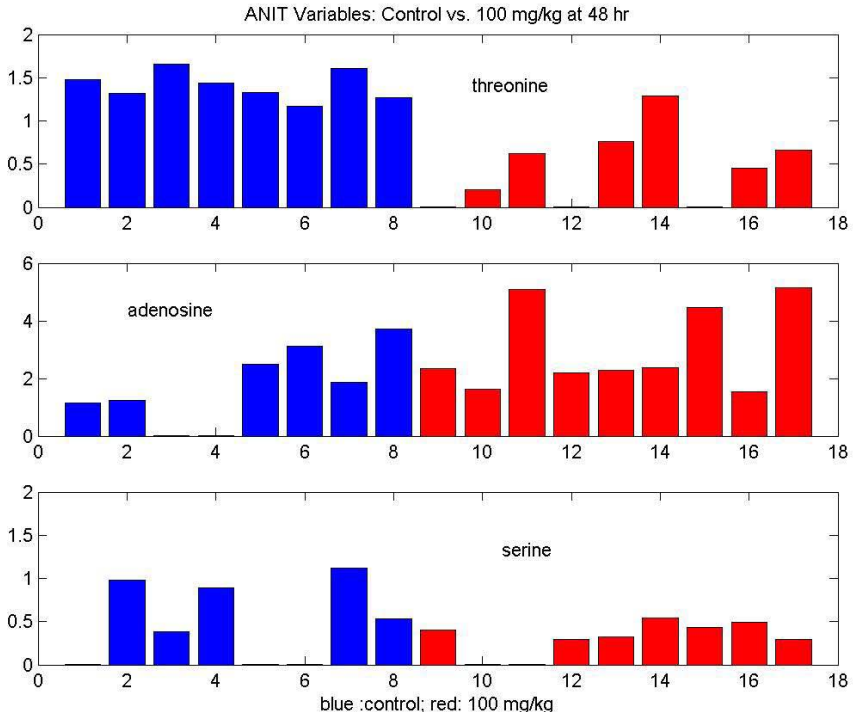

Figure 15: Normalized expressions for the variables tentatively identified by using the RT metabolite library.

It should be noted that the creatine candidate metabolite appears to be a clear marker even though it is only ranked number 362, and this illustrates the richness of the data set with respect to the number of potential markers that it contains. Furthermore, of the variables presented, creatine has a possible potassium adduct, citrate has possible sodium, potassium and ammonium adducts, and creatinine has a possible sodium adduct. Because these metabolite variables also have very high intensities, there is a high degree of confidence as to their identity. The other metabolites need to be investigated further, but it is hypothesized that the variables with intensities of order ten or higher are less likely to be numerical artifacts than the lower intensity compounds.

In addition to candidate metabolites tentatively identified from Harvard University's RT library, the identity of the other metabolites can be deduced. Specifically, evidence is presented in the analysis of the two-day 50 mg/kg data that two compounds from the bile acid biosynthesis pathway were up-regulated (i.e. glycocholate and taurocholate). Results indicate that these candidate metabolites can also be observed in the 100 mg/kg ANIT experiment (Figures 16 and 17).

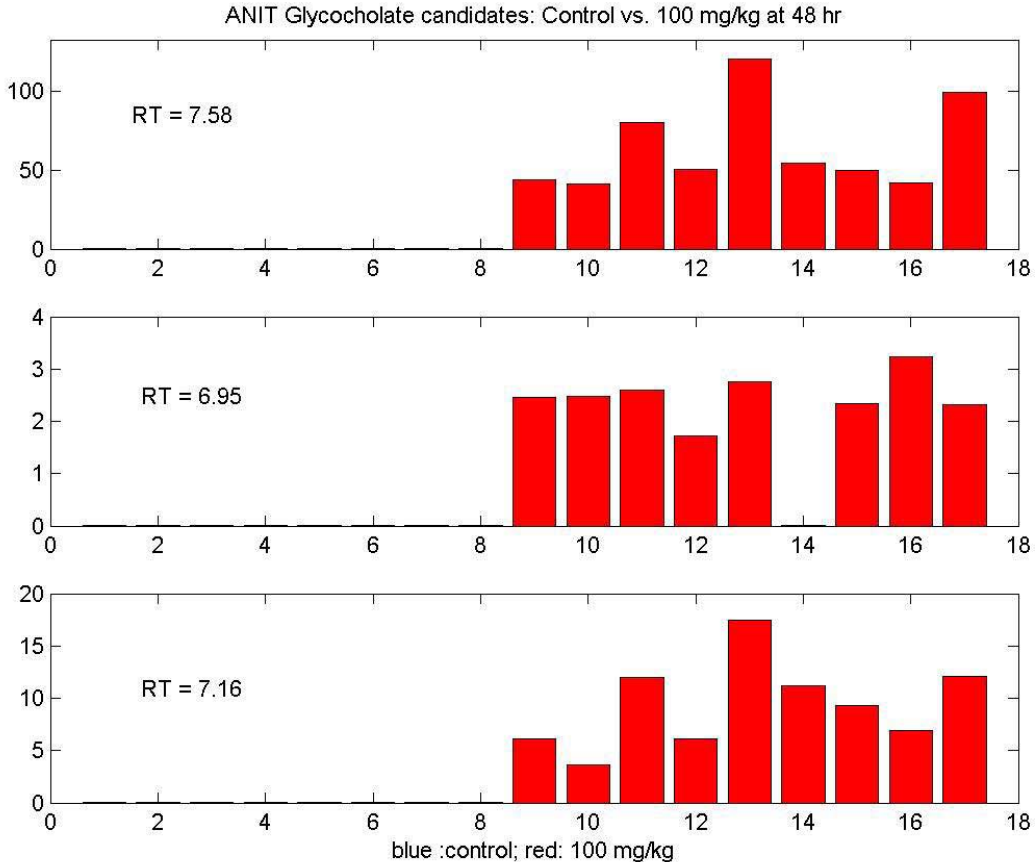

Figure 16: Intensity expression levels of three candidate metabolites (based on similar m/Z but differing RT) for glycocholate.

Data set is the normalized 3200 variable data table.

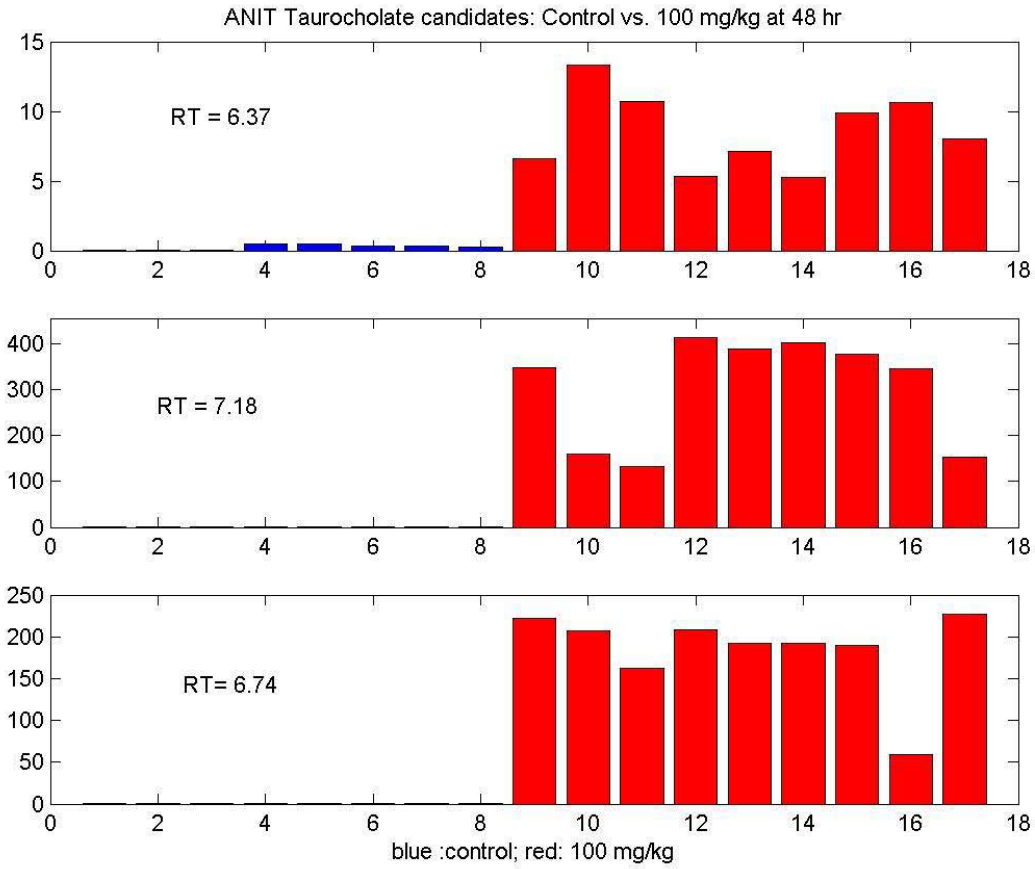

Figure 17: Intensity expression levels of three candidate metabolites (based on similar m/Z but different RT) for taurocholate.

Data set is the normalized 3200 variable data table.

It cannot be determined which of these candidate metabolites is the true compound without measuring the RTs of glycocholate and taurocholate standard metabolites. However, these higher intensity candidate biomarkers are more promising, and it should be noted that the taurocholate candidates with RT values of 7.18 and 6.74 both have possible adducts as does the glycocholate candidate with RT of 7.58. In an attempt to gain insight into the possible identification of these two bile acids, assuming an ionization by M^+H^+, a 20 ppm window was

opened around each m/Z and compared to each entry in a combined KEGG and METLIN database using a Matlab script for automatic mass matching. Many false positives were noted, and these can be eliminated only by constructing a RT database of pure metabolites. However, by searching for a combination of hypothetical metabolite species along with their adducts, we believe that we provide strong supporting evidence for identifying taurocholate and glycocholate as up-regulated biomarkers on the bile acid biosynthesis pathway.

Another potential candidate metabolite that was identified in this experiment was hippurate (Figure 18). As indicated above, this metabolite's identity should be confirmed by adding hippurate to the metabolite RT library. It should be noted that this metabolite is extremely interesting because it is unsaturated in spite of its high intensity and it has both possible sodium and potassium adducts. Thus, there is a high degree of confidence that it is some type of single-protonated marker regardless of its final identity. However, great care should be exercised in assigning this metabolite as a marker of ANIT toxicity because it is more than likely associated with gut microflora metabolism.

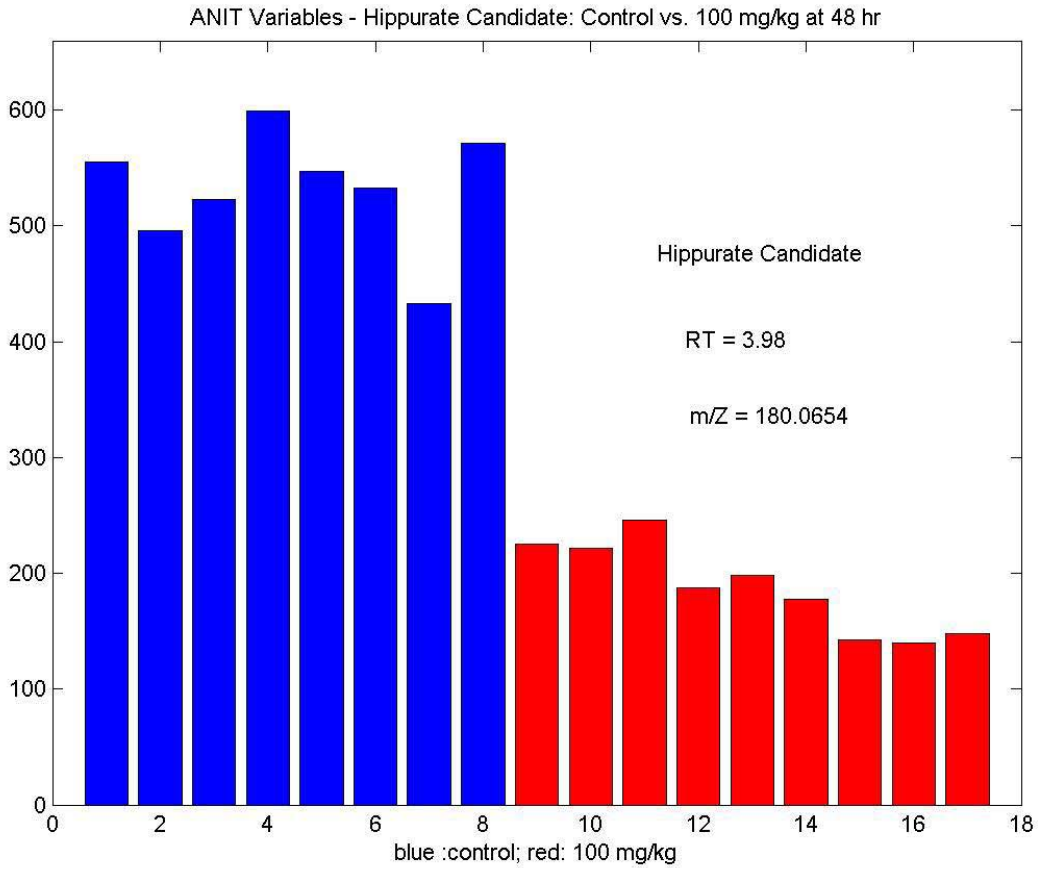

Figure 18: Intensity expression for the candidate metabolite hippurate with m/Z = 180.0654 and RT = 3.98

Although we have provided weaker evidence that hippurate, succinate, and 2-oxoglutarate metabolites have been identified in rat urine profiles from animals exposed to ANIT, their identities can be validated by including pure species of these metabolites in a RT database. Interestingly, by scanning the data matrix using Harvard University's RT database we have also identified the following additional compounds: L-tryptophan, L-leucine, serotonin, thiamine, 5-hydroxy-L-tryptophan, L-arginine, betaine, creatinine, L-threonine, L-phenylalanine, cytidylic acid, D-pyroglutamic acid, creatine, and 4-guanidinobutyric acid. However, none of

these were considered candidate biomarkers for ANIT exposure due to their low PLS-DA ranking.

An algorithm has been developed by Solutions Labs for matching data matrix variables with possible ($M^+ Na^+$, $M^+ K^+$, and $M^+ NH4^+$) adducts. This information was used, along with PLS-DA rankings, to surmise the potential existence of over one hundred ionic species that could prove useful as small molecule biomarkers of ANIT exposure. However, identifying these potential biomarkers will require using a large RT database.

4.0 CONCLUSION

In this study we examined the urinary metabolite profiles using both NMR-based and UPLC/MS-based metabonomics from rats following a single exposure to ANIT at various doses, and as a function of time post-dose. In toxicology, such dose-time metabonomics studies are important for an accurate determination of the severity of biological effects, and for biomarker identification that may be associated with toxicity. This study design enabled us to observe: 1) effects from vehicle solution (corn oil), 2) the onset and progression of ANIT-induced biological effects, and 3) the recovery process as a function of dose and time. Furthermore, this work expands upon other similar studies reported in the literature by investigating ANIT toxicity over a greater dose range (0.1 – 100 mg/kg) and time-course post-exposure.

The results present here demonstrated the greater sensitivity of both the NMR-based and UPLC/MS-based metabonomics, in conjunction with multivariate data analysis techniques, when compared with traditional clinical chemistry analysis for the detection of chemical exposure, the serial progression of the metabolic perturbations and recovery process, and the similarities and differences in metabolite profiles across ANIT doses.

The data from the present study suggests that NMR-based and UPLC/MS-based metabonomics are capable of detecting exposure to low doses of a classic cholestatic liver toxicant at levels below that observable by traditional methodologies (clinical chemistry and histopathology). These data correlate very well with an earlier biochemical study investigating abnormal lipoprotein metabolism, known to be associated with human hepatic cholestasis, following ANIT exposure in rats (Chisholm and Dolphin, 1996). This study showed that ANIT treatment induced a transient (maximal at day-two) and reversible hepatic cholestasis. In the present study, recovery from a single exposure began on day-three and showed a return towards pre-dose coordinates by day-four. The results presented in this study demonstrated the ability of NMR-based and UPLC/MS metabonomics to yield dose-response relationships that could be useful to probe for metabolite biomarkers of toxicity.

5.0 REFERENCES

Anthony[1] ML, Gartland KP, Beddell CR, Lindon JC, and Nicholson JK, "Studies of the biochemical toxicology of uranyl nitrate in the rat," *Archives of Toxicology*., **68,** 1, 1994 pp. 43-53.

Anthony[2] ML, Sweatman BC, Beddell CR, Lindon JC, and Nicholson JK, "Pattern recognition classification of the site of nephrotoxicity based on metabolic data derived from proton nuclear magnetic resonance spectra of urine," *Molecular Pharmacology*., **46,** 1, Jul 1994 pp. 199-211.

Beckwith-Hall BM, Nicholson JK, Nicholls AW, Foxall PJ, Lindon JC, Connor SC, Abdi M, Connelly J, and Holmes E, "Nuclear magnetic resonance spectroscopic and principal components analysis investigations into biochemical effects of three model hepatotoxins," *Chemical Research in Toxicology*., **11,** 4, Apr 1998 pp. 260-72.

Chisholm JW, and Dolphin PJ, "Abnormal lipoproteins in the ANIT-treated rat: a transient and reversible animal model of intrahepatic cholestasis," *Journal of Lipid Research*., **37,** 5, May 1996 pp. 1086-98.

Clayton TA, Lindon JC, Everett JR, Charuel C, Hanton G, Le Net JL, Provost JP and Nicholson JK, "Hepatotoxin-induced hypercreatinaemia and hypercreatinuria: their relationship to one another, to liver damage and to weakened nutritional status," *Archives of Toxicology*., **78,** 2, Feb 2004 pp. 86-96.

Dunn WB, and Ellis DI, "Metabolomics: Current analytical platforms and methodologies," *Trends in Analytical Chemistry*., **24,** 4, Apr 2005 pp. 285-94.

Fernie AR, Trethewey RN, Krotzky AJ, and Willmitzer L, "Metabolite profiling: from diagnostics to systems biology," *Nature Reviews: Molecular Cell Biology*., **5,** 9, Sep 2004 pp. 763-9.

Goldfarb S, Singer EJ, and Popper H, "Experimental cholangitis due to alpha-naphthyl-isothiocyanate (ANIT)," *American Journal of Pathology*., **40,** Jun 1962 pp. 685-98.

Holmes[1] E, Bonner FW, Sweatman BC, Lindon JC, Beddell CR, Rahr E, and Nicholson JK, "Nuclear magnetic resonance spectroscopy and pattern recognition analysis of the biochemical processes associated with the progression of and recovery from nephrotoxic lesions in the rat induced by mercury(II) chloride and 2-bromoethanamine," *Molecular Pharmacology*., **42,** 5, Nov 1992 pp. 922-30.

Holmes[2] E, Nicholson JK, Bonner FW, Sweatman BC, Beddell CR, Lindon JC, and Rahr E, "Mapping the biochemical trajectory of nephrotoxicity by pattern recognition of NMR urinalysis," *NMR in Biomedicine*., **5,** 6, Nov-Dec 1992 pp. 368-72.

Holmes[1] E, Nicholls AW, Lindon JC, Ramos S, Spraul M, Neidig P, Connor SC, Connelly J, Dament SJ, Haselden J, and Nicholson JK, "Development of a model for classification of toxin-induced lesions using 1H NMR spectroscopy of urine combined with pattern recognition," *NMR in Biomedicine*., **11,** 4-5, Jun-Aug 1998 pp. 235-44.

Holmes[2] E, Nicholson JK, Nicholls AW, Lindon JC, Connor SC, Polley S, and Connelly J, "The identification of novel biomarkers of renal toxicity using automatic data reduction techniques and PCA of proton NMR spectra of urine," *Chemometrics and Intelligent Laboratory Systems*., **44**, 1-2, Dec 1998 pp. 245-255.

Holmes[1] E, Nicholls AW, Lindon JC, Connor SC, Haselden JN, Damment SJ, Spraul M, Neidig P, and Nicholson JK, "Chemometric models for toxicity classification based on NMR spectra of biofluids," *Chemical Research in Toxicology*., **13,** 6, Jun 2000 pp. 471-8.

Holmes[2] E, and Shockcor JP, "Accelerated toxicity screening using NMR and pattern recognition-based methods," *Current Opinion in Drug Discovery & Development*., **3,** 1, Jan 2000 pp. 72-78.

Keun HC, Ebbels TM, Antti H, Bollard ME, Beckonert O, Schlotterbeck G, Senn H, Niederhauser U, Holmes E, Lindon JC, and Nicholson JK, "Analyticla reproducibility in (1)H NMR-based metabonomic urinalysis," *Chemical Research in Toxicology*., **15,** 11, Nov 2002 pp. 1380-6.

La S, Yoo HH, and Kim DH, "Liquid chromatography-mass spectrometric analysis of urinary metabolites and their pattern recognition for the prediction of drug-induced hepatotoxicity," *Chemical Research in Toxicology*., **18,** 12, Dec 2005 pp. 1887-96.

Lenz EM, Bright J, Wilson ID, Morgan SR, and Nash AF, "A 1H NMR-based metabonomic study of urine and plasma samples obtained from healthy human subjects," *Journal of Pharmaceutical and Biomedical Analysis*., **33,** 5, Dec 2003 pp. 1103-15.

Lindon JC, Nicholson JK, and Everett JR, "NMR Spectroscopy of Biofluids," *Annual Reports on NMR Spectroscopy*., **38,** 1999 pp. 1-88.

Lindon JC, Nicholson JK, Holmes E, Antti H, Bollard ME, Keun H, Beckonert O, Ebbels TM, Reily MD, Robertson D, Stevens GJ, Luke P, Breau AP, Cantor GH, Bible RH, Niederhauser U, Senn H, Schlotterbeck G, Sidelmann UG, Laursen SM, Tymiak A, Car BD, Lehman-McKeeman L, Colet JM, Loukaci A, and Thomas C, "Contemporary issues in toxicology the role of metabonomics in toxicology and its evaluation by the COMET project," *Toxicology and Applied Pharmacology*., **187,** 3, Mar 2003 pp. 137-46.

Lindon[1] JC, Holmes E, and Nicholson JK, "Metabonomics: systems biology in pharmaceutical research and development," *Current Opinion on Molecular Therapeutics*., **6,** 3, Jun 2004 pp. 265-72.

Lindon[2] JC, Holmes E, and Nicholson JK, "Toxicological applications of magnetic resonance," *Progress in Nuclear Magnetic Resonance Spectroscopy*., **45,** 1-2, Sep 2004 pp. 109-43.

Loo G, Goodman P, Hill KA, and Smith JT, "Creatine metabolism in the pyridoxine-deficient rat," *Journal of Nutrition*., **116,** 12, Dec 1986 pp. 2403-8.

Nicholson JK, Lindon JC, and Holmes E, "'Metabonomics': Understanding the metabolic responses of living systems to pathophysiological stimuli via multivariate analysis of biological NMR spectroscopic data," *Xenobiotica*., **29,** 11, Nov 1999 pp. 1181-9.

Nicholson JK, Connelly J, Lindon JC, and Holmes E, "Metabonomics: a platform for studying drug toxicity and gene function," *Nature Review: Drug Discovery*., **1,** 2, Feb 2002 pp. 153-61.

Nicholson JK, Holmes E and Wilson ID, "Gut microorganisms, mammalian metabolism and personalized health care," *Nature Reviews Microbiology.*, **3,** May 2005 pp. 431-438.

Plaa GL, and Priestly BG, "Intrahepatic cholestasis induced by drugs and chemicals," *Pharmacological Reviews*., **28,** 3, Sep 1976 pp. 207-73.

Reo NV, "NMR-based Metabolomics," *Drug and Chemical Toxicology*., **25,** 4, Nov 2002 pp. 375-82.

Roberston DG, Reily MD, Sigler RE, Wells DF, Paterson DA, and Braden TK, "Metabonomics: evaluation of nuclear magnetic resonance (NMR) and pattern recognition technology for rapid in vivo screening of liver and kidney toxicants," *Toxicological Sciences*., **57,** 2, Oct 2000 pp. 326-37.

Robertson DG, "Metabonomics in toxicology: a review," *Toxicological Sciences*., **85,** 2, Jun 2005 pp. 809-22.

Rozman KK, and Doull J. "General Principles of toxicology," in Environmental Toxicology, J Rose, Ed. Gordon and Breach Science, Amsterdam, 1998, pp 1-11.

Shockcor JP, and Holmes E, "Metabonomic applications in toxicity screening and disease diagnosis," *Current Topics in Medicinal Chemistry*., **2,** 1, Jan 2002 pp. 35-51.

Smilde AK, van der Werf MJ, Mijlsma S, van der Werff-van der Vat BJ, and Jellema RH, "Fusion of mass spectrometry-based metabolomics data," *Analytical Chemistry*., **77,** 20, Oct 2005 pp. 6729-36.

Uchida K, Ogura Y, Yamaga N, and Yamada K, "{alpha}-Naphthylisothiocyanate (ANIT) Induced Cholestasis in Rats," *Yonago Acta medica* **45,** 2002 pp. 59-68.

Waters NJ, Holmes E, Williams A, Waterfield CJ, Farrant RD, and Nicholson JK, "NMR and pattern recognition studies on the time-related metabolic effects of alpha-naphthylisothiocyanate on liver, urine, and plasma in the rat: an integrative metabonomic approach," *Chemical Research in Toxicology*., **14,** 10, Oct 2001 pp. 1401-12.

Waters NJ, Holmes E, Waterfield CJ, Farrant RD, and Nicholson JK, "NMR and pattern recognition studies on liver extracts and intact livers from rats treated with alpha-naphthylisothiocyanate," *Biochemical Pharmacology*., **64,** 1, Jul 2002 pp. 67-77.

GLOSSARY

2-OG – 2-oxoglutarate

AFB – Air Force Base

AFRL – Air Force Research Laboratory

ALKP - alkaline phosphatase

ALT - alanine aminotransferase

ANIT - alpha-naphthylisothiocyanate

AST - aspartate aminotransferase

BUN - urea nitrogen

°C – Celsius

CDFR(F344)/CrlBR – Fisher 344 rat strain

CREA - creatine

F344 – rat strain

fmol - femtomole

HPW/ RHPB – Human Performance Wing/ Research Human Performance and Biotechnology

Hz – hertz

IACUC - Institutional Animal Care and Use Committee

KEGG - **Kyoto Encyclopedia of Genes and Genomes**

kg – kilograms

LC - liquid chromatography

LDA - linear discriminant analysis

M – moles

METLIN – Metabolite Link Database

mg – milligram

Mhz – megahertz

mL – milliliter

mm - millimeters

mM – millimoles

MS - mass spectroscopy

ms – millisecond

m/z – mass to charge ratio

NMR – nuclear magnetic resonance

NOESY - Nuclear Overhauser Effect Spectroscopy

OPLS-DA – Orthogonal Partial Least Square-Discriminant Analysis

PAG - phenylacetylglycine

PC - principal components

PCA - principal component analysis

PLS-DA - partial least squares-discriminant analysis

ppm – parts per million

PTFE - polytetrafluoroethylene

Q-Tof - Quadrupole-Time of Flight

rpm – revolutions per minute

RT – retention time

s- seconds

SE - standard error

TMAO – trimethylamine oxide

TP – total protein

TSP - trimethylsilylpropionic (2, 2, 3, 3 d_4) acid

µL – microliter

V - voltage

UPLC - Ultra Performance Liquid Chromatograph